VIRGINIA POLYTECHNIC INSTITUTE
AND STATE UNIVERSITY

The Charles E. Via, Jr. Department
of Civil and Environmental Engineering
Blacksburg, VA 24061

Structural Engineering and Materials

VEHICULAR ACCESS DOORS UNDER HURRICANE FORCE WIND PRESSURE: ANALYSIS METHODS AND A DESIGN TOOL

by
Tian Gao
Graduate Research Assistant

Cristopher D. Moen, Ph.D., P.E.
Principal Investigator

Submitted to the:

Metal Building Manufacturers Association
1300 Sumner Ave
Cleveland, OH 44115-2851

Report No. CE/VPI-ST-11/02

August 2011

ACKNOWLEDGEMENTS

The authors are appreciative of the support they received from MBMA throughout this project, especially the thoughtful advice from the steering group. Mr. Jerry Hatch of NCI provided valuable guidance throughout the test program. Coordination with the sponsor was provided by Dr. Lee Shoemaker and Mr. Dan Walker of MBMA. Mr. Joe Hetzel of DASMA provided important input regarding access door design procedures and details. Dr. Ray Plaut, professor emeritus in the Civil and Environmental Engineering Department at Virginia Tech, assisted in the derivation of the elastica beam equations used to predict access door behavior.

TABLE OF CONTENTS

1.0 INTRODUCTION

1.1 RESEARCH MOTIVATION

It is essential that rolling sheet metal access doors in metal buildings, and the door jambs they are attached to, resist high pressures during an extreme wind event. Catastrophic damage to the building and its contents can occur if the door fails, as documented by recent post-hurricane surveys conducted after Hurricanes Ike and Katrina (FEMA 2005a; FEMA 2005b; RICOWI 2006; RICOWI 2007; RICOWI 2009). Once the door is breached, pressure accumulates inside the building that can fail the walls and roof (Figure 1). Estimated yearly damage from wind-induced damage in the U.S. is 5.4 billion dollars (NOAA 2011), reinforcing the need for reliable wind resistance structures and accurate wind design procedures.

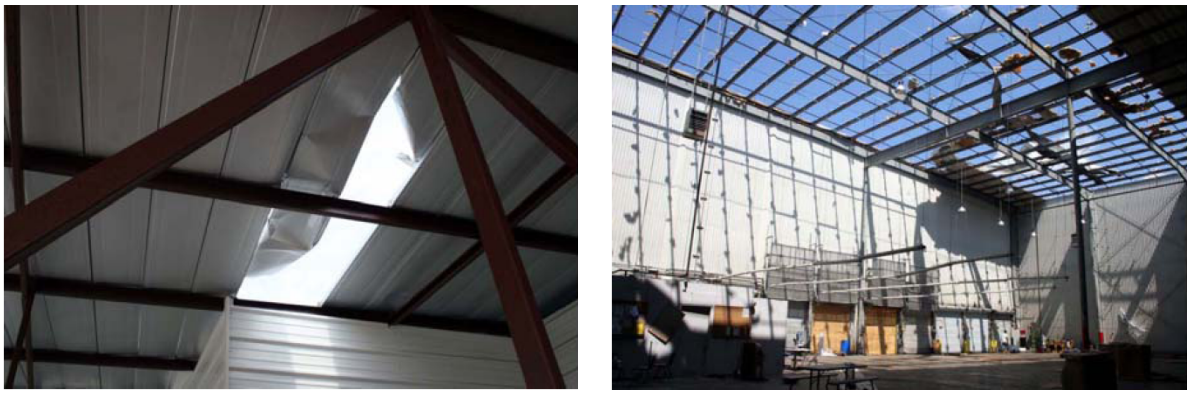

Figure 1. Metal building roof failures caused by internal wind pressure (RICOWI 2009)

1.2 ACCESS DOOR ANATOMY

The most common access door failure mode during a high wind pressure event is disengagement of the door from the track attached to the jamb as shown in Figure 2a (FEMA 2005). To avoid track disengagement in hurricane-prone regions, steel J-hooks called wind-locks (Figure 2b), are riveted to the door curtain and placed in tracks attached to the door jambs. The wind-locks float freely within the tracks during service, allowing the door to roll up and down. During an extreme wind event the curtain deflects out of plane, and the wind-locks engage a wind-bar attached to the door jambs (Figure 3, Section A-A). This engagement limits out-of-plane door deflection through the development of catenary forces that can overload the door jamb if not designed properly (Figure 2c).

The Door and Access Systems Manufacturers Association (DASMA) provides a method to predict wind-lock demand forces on door jambs, see Appendix A. This procedure calculates the wind pressure required to deflect the door enough to close the gap between the wind-lock and

wind-bar. Once the wind-locks have engaged, the geometry of the door is assumed fixed, i.e., there is no additional out-of-plane curtain deformation. Wind-lock reactions are calculated based on this fixed geometry with catenary equations and an evenly distributed pressure on the door.

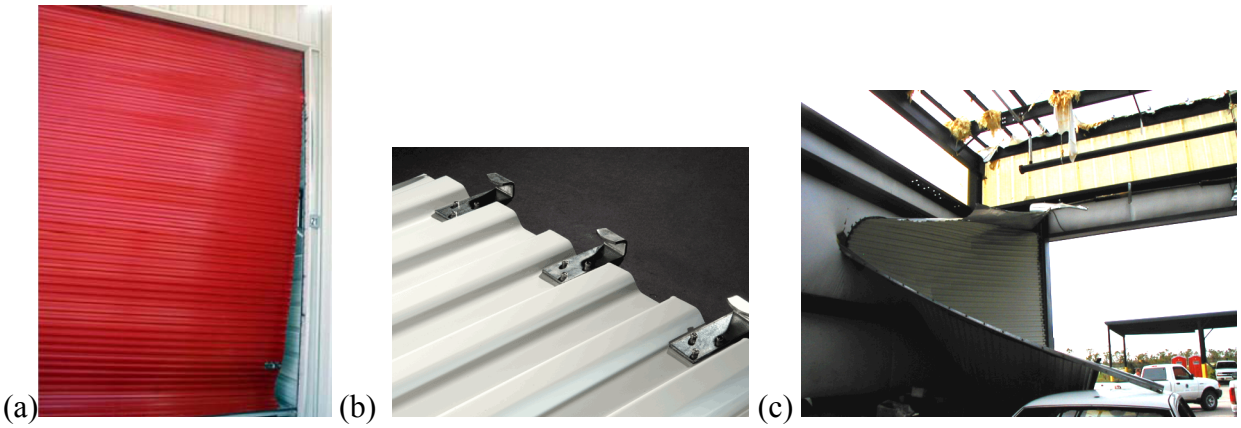

Figure 2. (a) Access door failure by disengagement of the door from the jamb track, (b) wind-locks, (c) jamb failure of an access door with wind-locks

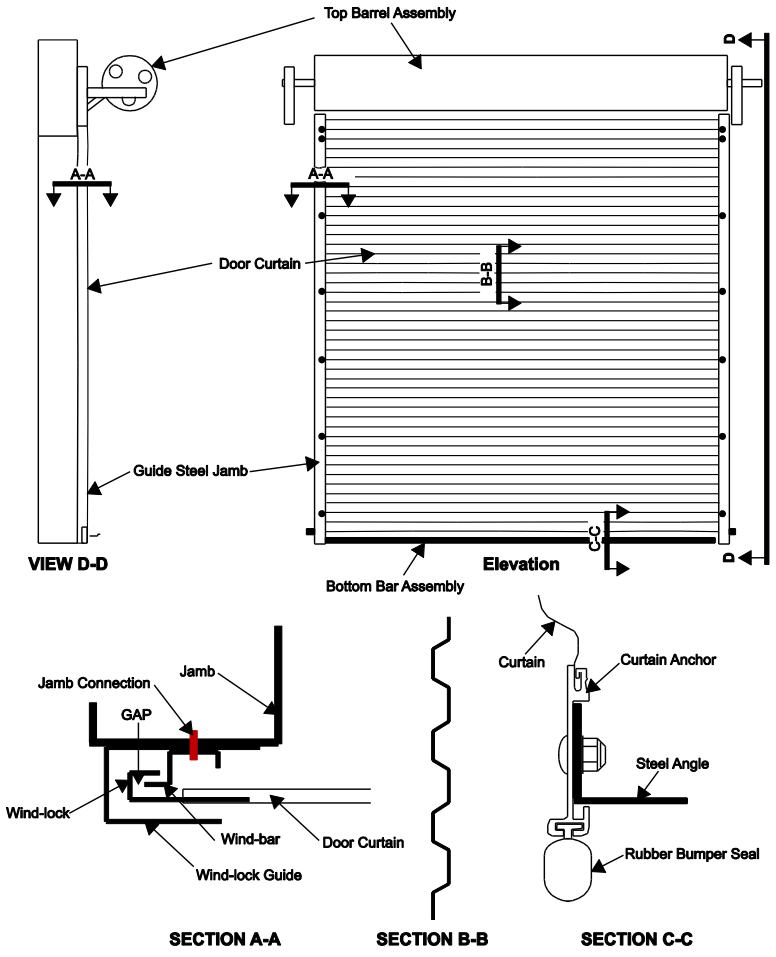

Figure 3. Typical access door details

1.3 ACCESS DOOR EXPERIMENTS

An experimental evaluation of the DASMA prediction equations for wind-lock force and door deflection was performed in 2009 (Gao and Moen 2009; Gao and Moen 2010). A 10 ft by 10 ft access door with wind locks was tested in both negative pressure (pulling door out of the building) and positive pressure (pushing the door into the building) with a custom vacuum chamber at DBCI in Douglasville, GA, see Figure 4a. The door had 18 wind locks along each vertical edge of the door, and the door jambs were cold-formed steel C-sections braced by Z-section girts (Figure 5). DBCI shop drawings for this door are provided in Appendix B.

Figure 4. (a) Rolling sheet metal door experiment, (b) Deformed jamb after test (Gao and Moen 2009)

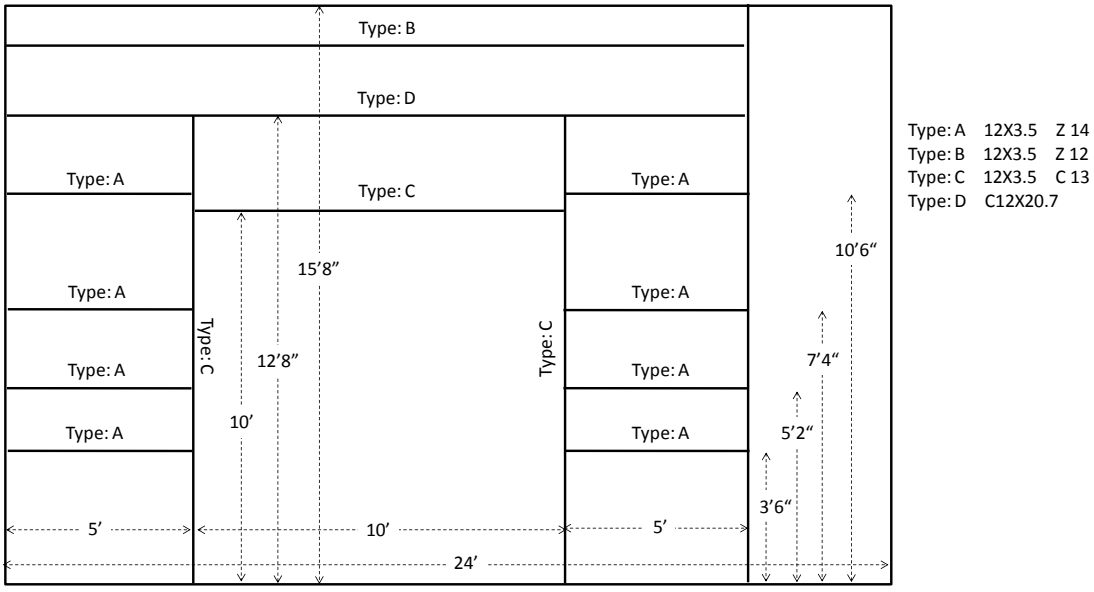

Figure 5. Cold-formed steel door framing (Gao and Moen 2009)

Each wind lock was instrumented with strain gauges, and strains were recorded as pressure was applied to the door. Maximum measured forces in the wind-locks were approximately 50% lower than that predicted by the DASMA procedure, compare 380 lbs per wind-lock in the experiments (Gao and Moen 2009) to 760 lbs per wind-lock predicted by DASMA at a pressure of 60 psf (see Appendix C). Measured out-of-plane door deflections were more than double that of the DASMA predictions, compare 12 in. (Gao and Moen 2009) to 5.3 in. predicted by DASMA (see Appendix C) at 60 psf.

The difference between the measured and predicted behavior was attributed to deflection of the cold-formed steel C-section jambs (Figure 4b), which accommodated additional in-plane movement of the door after the wind locks engaged. A small in-plane movement results in a large out-of-plane deformation, approximately 0.5 in. to 6 in. for the door studied in Douglasville. Therefore, as the C-section jamb deflected from the applied wind-lock forces, curtain deflection was amplified. The additional door deflection accommodated a funicular shape that reduced the in-plane component of the catenary force transferred to the door jamb. It was concluded from this experimental program that wind lock forces and door deflection are sensitive to jamb stiffness, and this stiffness should be included in a design approach for vehicular access doors. The DASMA design procedure was determined to be viable when the door jambs are rigid, however it underestimates door deflections and overestimates catenary forces for access doors with flexible door jambs.

1.4 RESEARCH STRATEGY

This research program aims to complement the existing DASMA access door wind analysis approach with a general procedure applicable to a wider range of access doors and jamb details, including doors attached to flexible jambs, e.g., cold-formed steel framing. The generalized analysis procedures are founded on an analytical framework of nonlinear Euler-Bernoulli elastica differential equations. Jamb stiffness boundary conditions are approximated with hand calculations employing existing cantilever and torsional stiffness engineering expressions. The analytical framework is validated with thin-shell finite element modeling and the Douglasville experimental data, and then implemented as a custom built, freely available Matlab program. The elastica analytical framework is introduced in the following section.

2.0 ANALYTICAL FRAMEWORK

2.1 FORMULATION

The access door experiments in Douglasville, GA (Gao and Moen 2009) demonstrated that away from the top and bottom of the door, curtain deflections due to wind pressure resulted in primarily one-way deformation across the span of the door. If one-way action is assumed, the prediction of catenary forces and deflections in a vehicular access door can be simplified to an inextensible beam strip model like that shown in Figure 6. This assumption is consistent with the existing DASMA prediction approach, except translational springs have been added to the beam ends to simulate door jamb flexibility.

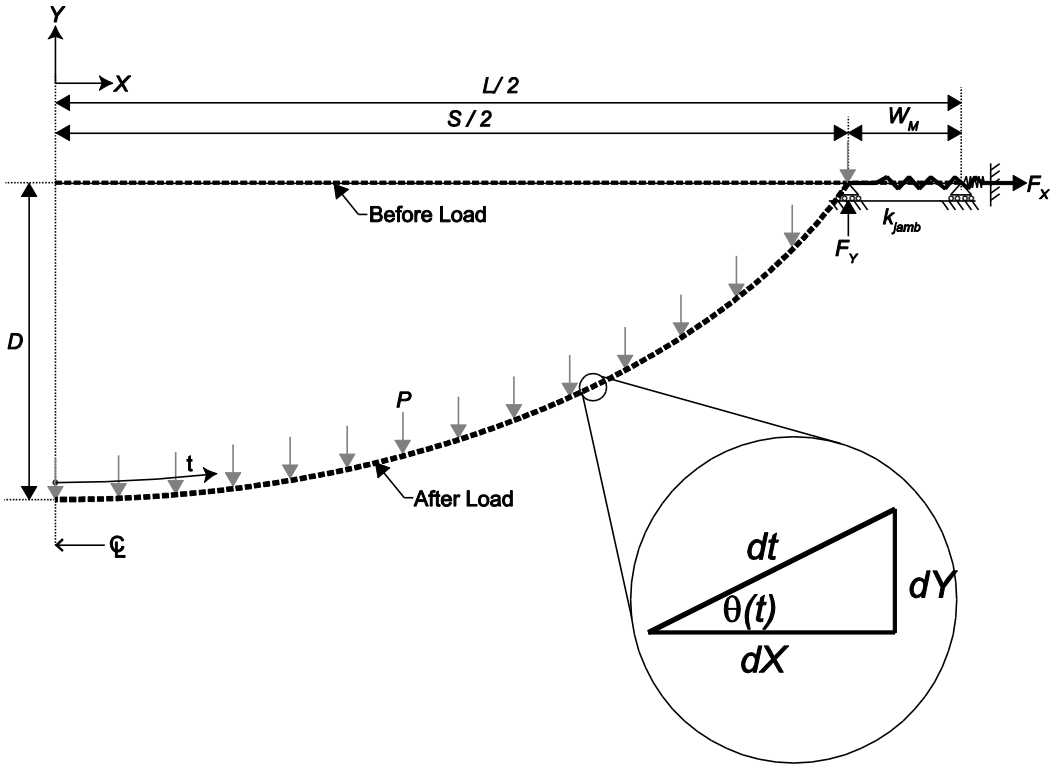

Figure 6. Curtain strip model notation

Beam strip behavior can be represented with the elastica solution for beams, which employs Euler-Bernoulli beam theory and accommodates large flexural deformations (Timoskenko and Gere 1961). Shear deformations are neglected. Defining X and Y as the door's deflected shape in Cartesian coordinates, t as the curvilinear distance along the curtain, and the slope of the door curtain as $\theta(t)$, the change in X and Y at location t is

$$X(t)' = cos(\theta(t)) \quad (1)$$

$$Y(t)' = \sin(\theta(t)), \tag{2}$$

where t is a relative indicator of position over the half span ranging from 0 to 1.

Summing the changes in X and Y by integrating Eqs. (1) and (2) results in expressions for the deflected shape as a function of t

$$X(t) = \int_0^t \cos(\theta(t))dt \tag{3}$$

$$Y(t) = \int_0^t \sin(\theta(t))dt\,. \tag{4}$$

Euler-Bernoulli beam theory dictates that the beam moment $M(t)$ is proportional to curvature $d\theta(t)/dt$ and flexural rigidity EI as given by

$$\theta(t)' = \frac{M(t)}{EI}\,. \tag{5}$$

For a vehicular access door, the moment of inertia, I, would be calculated with the height of door attributed to one wind-lock, i.e., a tributary width as shown in Figure 7.

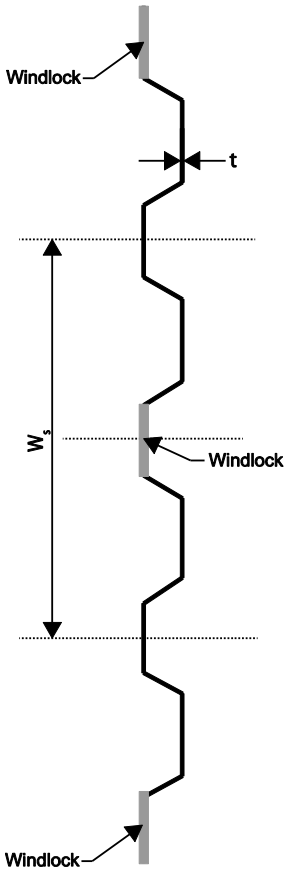

Figure 73. Windlock tributary distance W_s is 6.5 in. for DBCI Series 5000 test door

The relationship between slope $\theta(t)$ and moment $M(t)$ is obtained by integrating Eq. (5)

$$\theta(t) = \int_0^t \frac{M(t)}{EI} dt \,, \tag{6}$$

and the beam shear, $V(t)$, is calculated as the derivative of the moment

$$\theta(t)'' = M(t)' = V(t) \,. \tag{7}$$

Beam shear $V(t)$ is equilibrated with components of the uniform pressure P and horizontal reaction F_X as shown in Figure 8

$$V(t) = M(t)' = [-P\cos(\theta(t)) + F_X \sin(\theta(t))] \,, \tag{8}$$

leading to an equation for moment along the door curtain as a function of pressure P and spring force F_X

$$M(t) = \int_0^t [-P\cos(\theta(t)) + F_X \sin(\theta(t))]\, dt \,. \tag{9}$$

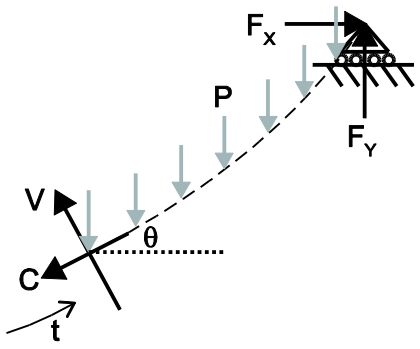

Figure 8. Free body diagram, support reaction (F_X, F_Y), internal beam cut (V, C)

The horizontal reaction F_X is related to the jamb stiffness k_{jamb} and the X displacement. The jamb stiffness is assumed to be bi-linear, i.e., zero before the jamb engages and k_{jamb} after the door deflects enough to close the gap between the wind-lock and the wind-bar, W_{GAP}

$$F_X = 0 \,,\; W_M < W_{GAP} \tag{10}$$

$$F_X = k_{jamb}\left(W_M - W_{GAP}\right) \,,\; W_M \geq W_{GAP}. \tag{11}$$

2.2 GOVERNING EQUATIONS

To accommodate the statement of governing equations for the elastica beam problem and to simplify their numerical solution, the following non-dimensional quantities are defined

$$x = \frac{X}{L/2} \tag{12}$$

$$y = \frac{Y}{L/2} \tag{13}$$

$$m = \frac{MS}{2EI} \tag{14}$$

$$v = \frac{V(L/2)^2}{EI} \tag{15}$$

$$f_X = \frac{F_X(L/2)^2}{EI} \tag{16}$$

$$p = \frac{P(L/2)^3}{EI} \tag{17}$$

$$k = \frac{k_{jamb}(L/2)^3}{EI} \tag{18}$$

$$w_{GAP} = \frac{W_{GAP}}{L/2} \tag{19}$$

The nondimensional forms of the governing equations, i.e., Eqs. (1), (2), (5), and (8), can then be written as:

$$x(t)' = cos(\theta(t)) \tag{20}$$

$$y(t)' = sin(\theta(t)) \tag{21}$$

$$\theta(t)' = m(t) \tag{22}$$

$$m(t)' = [- ptcos(\theta(t)) + f_X sin(\theta(t))] \ . \tag{23}$$

2.3 INITIAL CONDITIONS

The solution of the governing equations required four initial conditions. The beam is simply-supported at its ends, and therefore the moment *m* at the beam end is zero

$$\mathrm{m}(1) = 0 \, . \tag{24}$$

The beam has zero slope at midspan, i.e.,

$$\theta(0) = 0 \, . \tag{25}$$

Out-of-plane deflection is restricted (roller support) at the beam ends, and therefore

$$y(1) = 0 \,. \tag{26}$$

The in-plane displacement at the beam end is

$$x(1) = 1 - \frac{f_X}{k} - w_{GAP} \,. \tag{27}$$

2.4 SOLUTION

This nonlinear system of ordinary differential equations is a boundary value problem. Eqs. (20) to (23) can be numerically integrated with the function *bvp4c* in Matlab (Matlab 2011a), resulting in the displacements, slope, and moment along the beam. See Appendix D for the coded implementation. An example of the Matlab predicted door deflection with increasing pressure and including wind-lock engagement is shown in Figure 9. These beam strip results will be validated with the Douglasville experiments and full scale finite element simulations after simplified methods for predicting jamb stiffness (k_{jamb}) are derived in the following section.

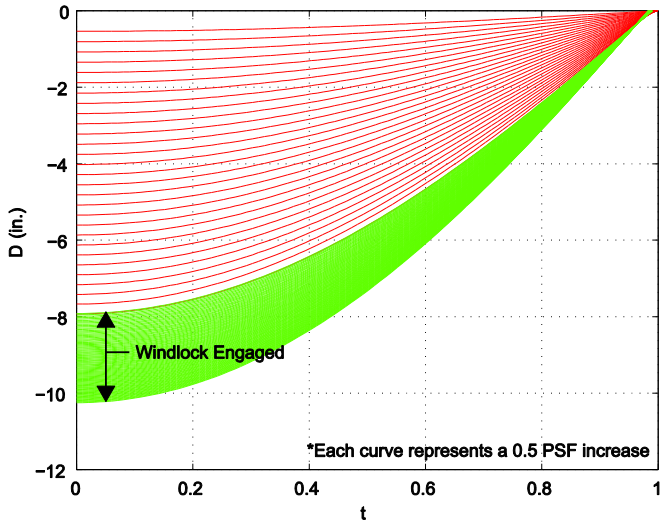

Figure 9. Door deflection using curtain beam strip analytical framework

3.0 FLEXIBLE JAMB STIFFNESS PREDICTION

3.1 TYPICAL JAMB DETAILS

Vehicular access door jamb details vary widely from manufacturer to manufacturer and building to building. The wind-bar may be screw-fastened to a hot-rolled steel jamb (Figure 10a) or a cold-formed steel C-section (Figure 2). Another common detail is to use sleeve anchors to fasten the wind-bar directly to a masonry wall (Figure 10b). A rational assumption when using the beam strip approach with a masonry wall or a hot rolled section would be to set $k_{jamb}=\infty$. For a cold-formed steel framing system, the selection of k_{jamb} is more difficult and requires calculation.

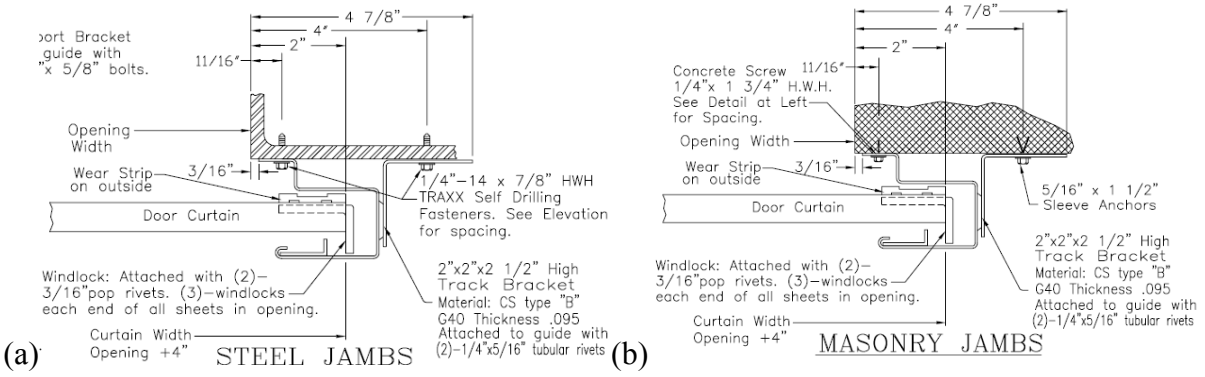

Figure 10. Door jamb details - (a) hot-rolled steel and (b) masonry (Allen 2008)

In this chapter, a prediction method is presented for calculating the in-plane stiffness of flexible door jambs, and specifically, jambs constructed from open cross-section cold-formed steel structural members, e.g., Cee and Zee sections. The goal is to develop a hand calculation method that an engineer could use to approximate k_{jamb}. The approach is based on the jamb details encountered in the experimental program (Section 1.3), however the equations are formulated to be general with the goal of accommodating a broad range of cold-formed steel framing details.

3.2 PREDICTION METHOD

Jamb stiffness in the plane of the door (X direction) can be approximated by assuming that the jamb behaves as two springs in series, one spring representing in-plane stiffness dictated by cross-section bending, k_b, shown in Figure 11a, and the other representing in-plane stiffness from jamb twist, k_t, as shown in Figure 11b. The total in-plane jamb stiffness k_{jamb} is

$$k_{jamb} = \left(\frac{1}{k_b} + \frac{1}{k_t} \right)^{-1} . \tag{28}$$

When a very flexible spring is in line with a very stiff spring, then the form of Eq. (28) dictates that the very flexible spring will govern system stiffness. For example, when the jamb is very flexible in torsion, i.e., an open cross-section with only a few girts bracing the jamb along the wall, then k_{jamb} will be similar in magnitude to k_t. The following sections provide guidelines for calculating k_t and k_b.

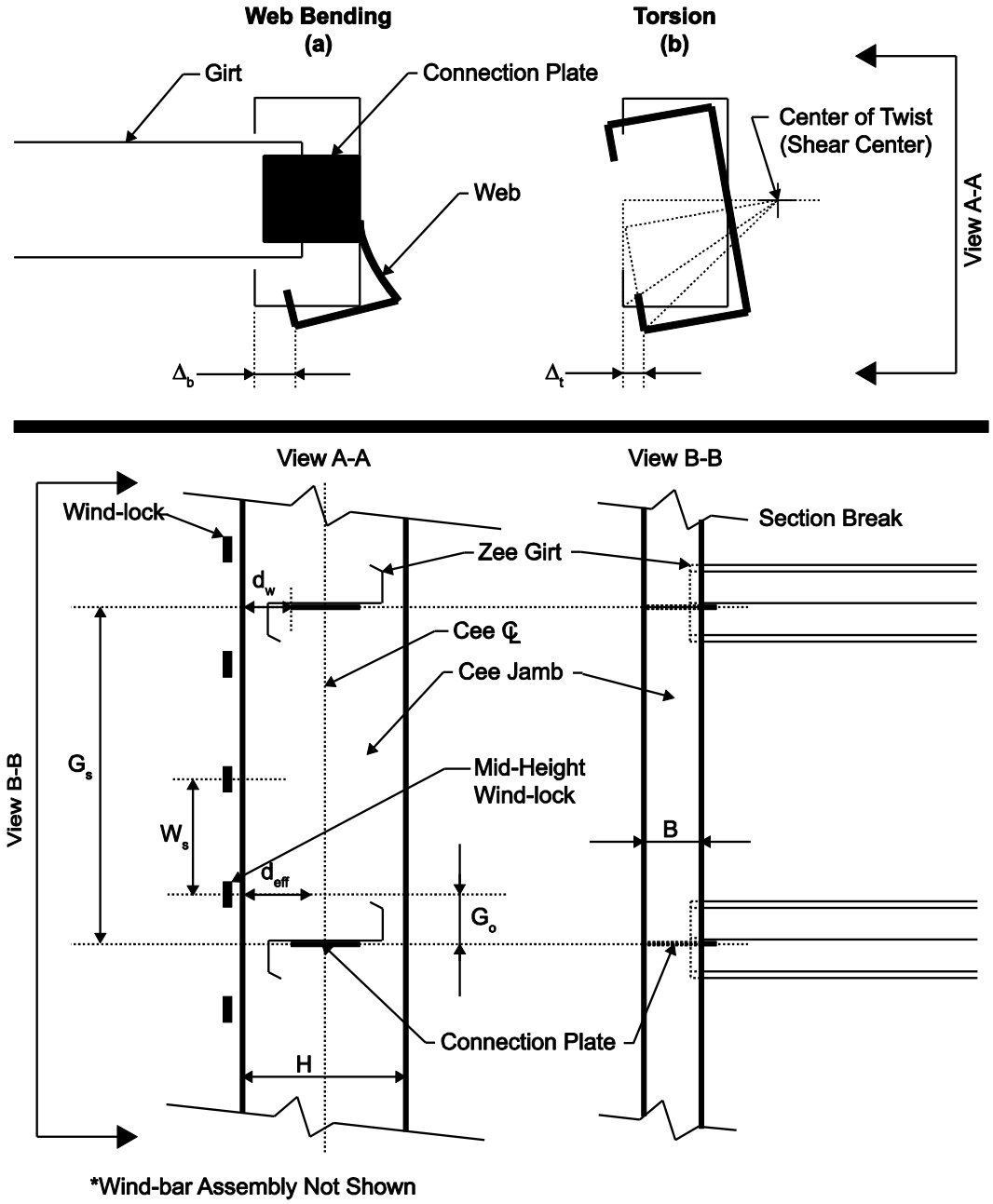

Figure 114. Jamb flexibility occurs from (a) cross-section bending and (b) cross-section twist. Note that d_{eff} is the effective web bending distance at the location where stiffness is being calculated, i.e. G_o.

3.3 SECTION WEB BENDING

The in-plane jamb flexibility contribution from bending deformation of open cold-formed steel cross-sections can be approximated by using the same "springs in series" analogy discussed in the previous section, except now the two springs represent web flexural stiffness, k_{bp}, and web rotational stiffness, k_{bm}

$$k_b = \left(\frac{1}{k_{bp}} + \frac{1}{k_{bm}} \right)^{-1}. \tag{29}$$

In the following derivations, it is assumed that the dominant reaction affecting jamb stiffness is the in-plane component F_x (see Figure 12). Using a cantilever model for the web with a point load at the tip in the direction of F_x

$$k_{bp} = \frac{3EI_w}{\left(d_{eff}\right)^3}, \tag{30}$$

where I_w is the sheet curtain moment of inertia over the tributary width, W_s, of a wind-lock (see Figure 7)

$$I_w = \frac{1}{12} W_s t^3, \tag{31}$$

and t is the jamb base metal thickness. The length of the cantilever, d_{eff}, is assumed to be an effective web length linearly varying from d_w if the wind-lock is located at the girt, to $H/2$ if the wind-lock under consideration is located far from the girts (see Figure 11)

$$d_{eff} = \left(\frac{G_o}{G_s} \right) \left(H - d_w/2 \right) + d_w \quad , 0 \leq G_o \leq G_s/2. \tag{32}$$

The location of the wind-lock being studied relative to the nearest girt is G_o, and the girt spacing is G_s as shown in Figure 11.

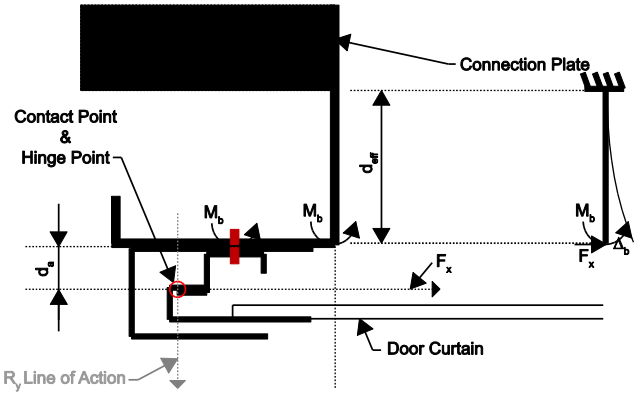

Figure 12. Jamb cross-section stiffness notation

The out-of-plane jamb web displacement associated with the moment $M_b=F_x d_a$ is

$$\Delta_{bm} = \frac{M_b \left(d_{eff}\right)^2}{2EI_w} = \frac{F_x d_a \left(d_{eff}\right)^2}{2EI_w} \tag{33}$$

where d_a is the moment arm between the F_X component of the wind-lock force and the jamb (Figure 12). Rearranging Eq. (33) such that $k_{bm}=F_X/\Delta_{bm}$, then

$$k_{bm} = \frac{2EI_w}{d_a \left(d_{eff}\right)^2}. \tag{34}$$

3.4 JAMB TWIST

Wind-lock forces can apply torsion to a door jamb, resulting in twist that affects in-plane system flexibility, i.e., k_{jamb}. For most practical cases, the jamb torsional stiffness, k_t, in Eq. (28) is expected to be much higher than k_b, especially because one flange of a cold-formed steel jamb will typically be through-fastened to the exterior metal sheeting of the building. For this case, $k_t=\infty$ is a reasonable assumption that can be made at the discretion of the engineer.

When k_t is expected to have an impact on jamb stiffness, it can be approximated with existing equations in AISC Design Guide 9: Torsional Analysis of Structural Steel Members (AISC 2003). The equations include the St. Venant torsional constant, J, and the warping torsion constant, C_w, both of which are tabulated for typical SSMA cross-sections (SSMA 2010), and which can be calculated for any general open thin-walled cross section with freely available section property calculators, e.g., CUFSM (Schafer and Ádány 2006).

If twist and warping are assumed fixed between girts as shown in Figure 13, and the wind-lock forces are assumed to act as a continuous torsion per unit length on the girt, then the twist angle, θ, at any location z between 0 and G_s is

$$\theta(z) = \frac{T_j G_s \left(EC_w/GJ\right)^{0.5}}{2GJ} \left[\begin{array}{l} \left(\dfrac{1+\cosh\left(\dfrac{G_s}{\left(EC_w/GJ\right)^{0.5}} \right)}{\sinh\left(\dfrac{G_s}{\left(EC_w/GJ\right)^{0.5}} \right)} \right) \left(\cosh\left(\dfrac{z}{\left(EC_w/GJ\right)^{0.5}} \right) - 1.0 \right) + \\ \dfrac{z}{\left(EC_w/GJ\right)^{0.5}} \left(1 - \dfrac{z}{G_s}\right) - \sinh\left(\dfrac{z}{\left(EC_w/GJ\right)^{0.5}} \right) \end{array} \right]. \tag{35}$$

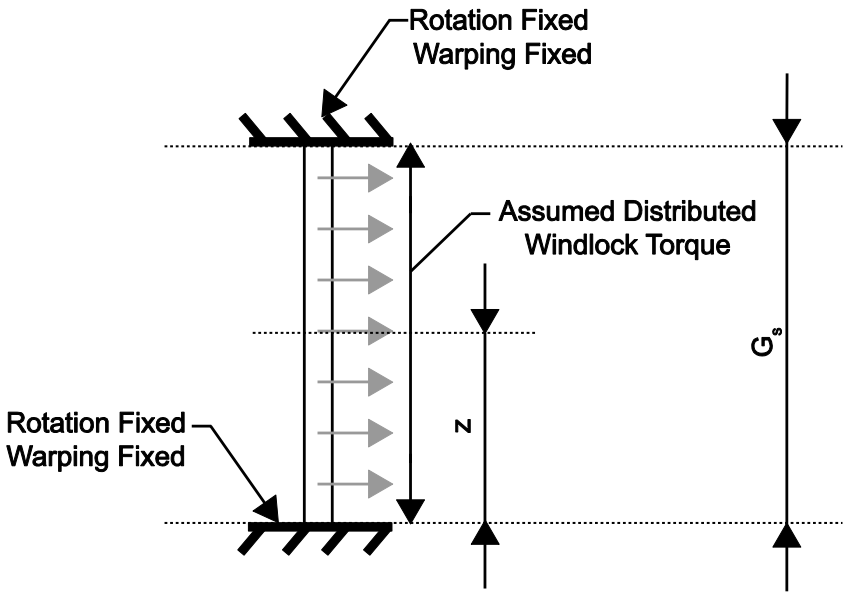

Figure 13. Jamb assumed as twist fixed warping fixed between girts

To approximate k_t at a specific wind-lock location $z=G_o$, the angle of twist at $\theta(z=G_o)$ is calculated with Eq. (35), where T_j is a torsion per unit length from a unit force per length in the direction of F_x, about the cross-section's center of twist, i.e., its shear center, as shown in Figure 14

$$T_j = 1\left(\frac{H}{2} + d_a\right). \tag{36}$$

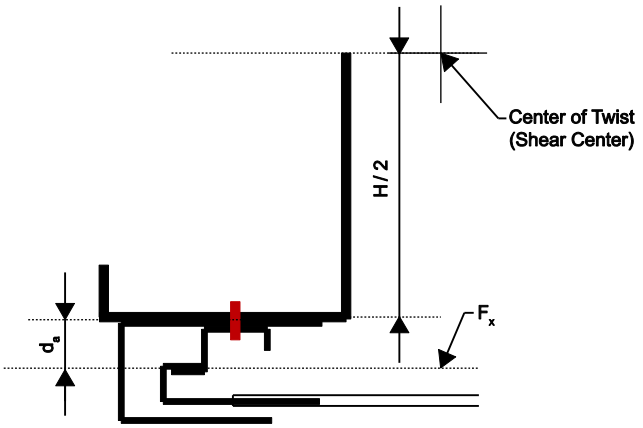

Figure 14. Torsion is created by the wind-lock force acting about the cross-section center of twist

The angle of twist at the wind-lock location can be converted into a displacement, Δ_t, shown in Figure 15 by substituting $\theta=\theta(G_o)$ into

$$\Delta_t = L_t \cos\left(\theta_a\right) - L_t \cos\left(\theta_a + \theta\right) \tag{37}$$

where

$$\theta_a = \sin^{-1}\left(\frac{H/2 + d_a}{L_t}\right) \tag{38}$$

and

$$L_t = \sqrt{\left(\frac{H}{2} + d_a\right)^2 + \left(x_o + B_w\right)^2}\ . \tag{39}$$

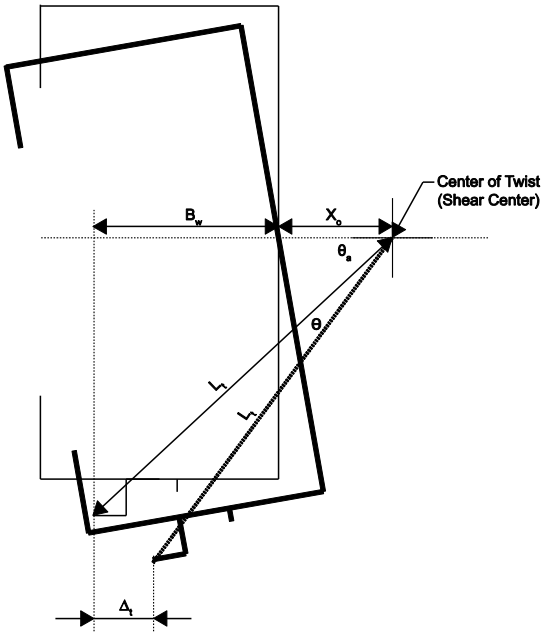

Figure 15. Cross section twist geometry

The torsional stiffness, k_t, at the location $z=G_o$ is calculated as a unit force causing the displacement Δ_t, i.e.,

$$k_t = \frac{1}{\Delta_t}\ . \tag{40}$$

Torsional stiffness, as represented by Eq. (40), varies along the length of the jamb. When a wind-lock is near a girt connection, i.e., near the fixed support in Figure 11, Δ_t will be small, resulting in a high k_t. Vice versa, if the wind-lock under consideration is far from the girt support, then Δ_t will increase, resulting in a decrease in k_t. The cumulative jamb stiffness, i.e., k_{jamb}, is calculated for the door system in the Douglasville experiments in the next section using this simplified approach.

3.5 EXAMPLE – DOUGLASVILLE EXPERIMENTS

Jamb stiffness is approximated for the tested door system described in Section 1.3. The stiffness is calculated at the wind-lock positioned at mid-height of the door, which is 2.0 in. from the nearest girt, i.e., G_o=2.0 in. as shown in Figure 16. Pertinent dimensions required to calculate k_{jamb} are summarized in Table 1.

Table 1. Listing of input parameters for Experimental door jamb stiffness calculation

Input	Value	Units	Note
B	3.5	in.	width of flange
B_w	2.44	in.	distance to hinge point
H	12.00	in.	depth of Cee
d_a	0.94	in.	depth of wind-bar
d_w	3.66	in.	as measured on test door
G_s	20	in.	spacing of girt
G_o	2	in.	include allowance for connection plate thickness
x_o	1.450	in.	distance from web to shear center
J	0.007098	in^4	St. Venant torsion constant (SSMA)
C_w	92.672	in^6	warping torsion constant (SSMA)
t	0.1017	in.	thickness of base metal
E	30,000	ksi	elastic modulus
G	11,200	ksi	shear modulus
z	2.00	in.	torsion analysis location (middle wind-lock)

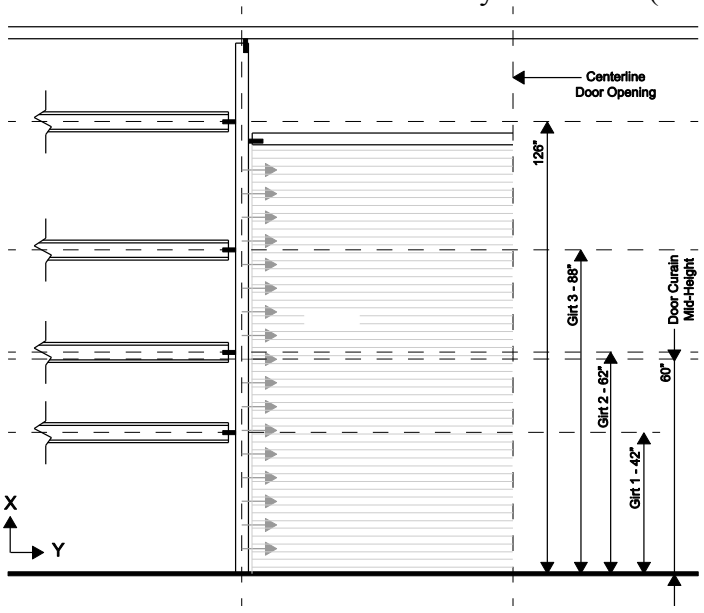

Figure 165. Test door dimensions (Gao and Moen 2009)

Test Door Jamb Stiffness Example

- obtain section constants from SSMA table

$J := 0.007098\ in^4$ $C_w := 92.672\ in^6$ $d_w := 3.66\ in$ $B := 3.5\ in$ $x_o := 1.450\ in$

$t := 0.1017\ in$ $H := 12.00\ in$ $d_a := 0.94 + .097\ in$ $B_w := 2.52\ in$

- apply steel material properties

$E := 30000\cdot 1000\ psi$ $G := 11200\cdot 1000\ psi$

- calculate windlock tributary area

$W_s := 6.5\ in$

- determine torsional support length

$G_s := 20\ in$ $G_o := 2.0\ in$ *middle windlock offset including connection plate thickness

$$T_j := 1\left(\frac{H}{2} + d_a\right) = 7.037 \quad \frac{lb - in}{in}$$ *unit Fx force distributed over windlock tributary distance

$$\theta(z) := \frac{T_j \cdot G_s \cdot \sqrt{\frac{E\cdot C_w}{G\cdot J}}}{2G\cdot J} \cdot \left[\frac{1 + \cosh\left(\frac{G_s}{\sqrt{\frac{E\cdot C_w}{G\cdot J}}}\right)}{\sinh\left(\frac{G_s}{\sqrt{\frac{E\cdot C_w}{G\cdot J}}}\right)} \left(\cosh\left(\frac{z}{\sqrt{\frac{E\cdot C_w}{G\cdot J}}}\right) - 1.0\right) \ldots \right.$$
$$\left. + \frac{z}{\sqrt{\frac{E\cdot C_w}{G\cdot J}}} \cdot \left(1 - \frac{z}{G_s}\right) - \sinh\left(\frac{z}{\sqrt{\frac{E\cdot C_w}{G\cdot J}}}\right) \right]$$ **Eq. (36)**

- determine z at location of middle windlock

$z := G_o$

$\theta := \theta(z) = 1.3665 \times 10^{-7}$ radians

- determine jamb stiffness from torsion

$$L_t := \sqrt{\left(\frac{H}{2} + d_a\right)^2 + \left(x_o + B_w\right)^2} = 8.0796\ in$$ **Eq. (39)**

$$\theta_a := \operatorname{asin}\left[\frac{\left(\frac{H}{2}\right) + d_a}{L_t}\right] = 1.0571 \quad \text{rad} \qquad \theta_a \cdot \frac{180}{\pi} = 60.57$$ **Eq. (38)**

$$\Delta_t := L_t \cdot \cos(\theta_a) - L_t \cdot \cos(\theta_a + \theta) = 9.6162 \times 10^{-7} \quad \text{in}$$ **Eq. (37)**

$$k_t := \frac{1}{\Delta_t} = 1.0399 \times 10^{6} \quad \frac{\text{lb}}{\text{in}} \quad \text{per windlock Fx}$$ **Eq. (40)**

- determine jamb web bending stiffness

$$b := 1 \qquad h := t$$

$$I_w := \frac{b \cdot h^3}{12} = 8.7656 \times 10^{-5} \ \text{in}^4$$ **Eq. (31)**

- determine web moment of inertia per windlock tributary area

$$I_w := I_w \cdot W_s = 5.6976 \times 10^{-4} \quad \text{in}^4$$

$$d_{eff} := \frac{\frac{H}{2} - d_w}{\frac{G_s}{2}} \cdot G_o + d_w = 4.128 \ \text{in}$$ *average web local distance allowed for web bending **Eq. (32)**

$$k_{bp} := \frac{3 \cdot E \cdot I_w}{d_{eff}^{3}} = 728.9847 \quad \frac{\text{lb}}{\text{in}}$$ **Eq. (30)**

$$k_{bm} := \frac{2 \cdot E \cdot I_w}{d_a \cdot (d_{eff})^2} = 1.9346 \times 10^{3} \quad \frac{\text{lb}}{\text{in}}$$ **Eq. (34)**

- therefore, the jamb web bending stiffness is

$$k_b := \left(\frac{1}{k_{bp}} + \frac{1}{k_{bm}}\right)^{-1} = 529.4711 \quad \frac{\text{lb}}{\text{in}} \quad \text{per windlock Fx}$$ **Eq. (29)**

- total jamb bending stiffness is

$$k_{jamb} := \left(\frac{1}{k_b} + \frac{1}{k_t}\right)^{-1} = 529.2016 \quad \frac{\text{lb}}{\text{in}} \quad \text{per windlock Fx}$$ **Eq. (28)**

It is concluded from the previous example that cross-section bending controls the jamb stiffness for the wind-lock considered because of its close proximity to a girt. The calculated jamb stiffness, k_{jamb}=529 lb/in., will be used in the following validation section to compare the beam strip model predictions to finite element simulations and experimental results.

4.0 BEAM STRIP MODEL VALIDATION

The beam strip model developed in Chapter 2 provides a computational efficient approximate method for predicting access door deflections and catenary forces. Up to this point, the method's inherent assumption of 2D beam strip behavior is based primarily on observations from the experimental program. To gain a more thorough understanding of access door behavior, a 3D finite element modeling protocol is developed and validated in this chapter. The protocol accommodates more detailed study of boundary condition effects, pressure loading types, and even the effect of the stiffening angle often present spanning across the bottom of an access door. The finite element modeling protocol is used to demonstrate that the beam strip model is a viable approach for predicting door deflections and catenary forces. A custom Matlab finite element model generator was developed, which can produce and run 100s of finite element models for use in parameter studies. The Matlab code could be useful for future work involving other door geometries and jamb stiffnesses.

4.1 FE MESHING

The modeling protocol employs the commercial finite element code ABAQUS (ABAQUS 2010). The general four node S4 element was chosen based on studies summarized in Appendix E. The finite element mesh was generated with custom Matlab code that accepts the sheet curtain cross-section dimensions as input and extrudes the sheet curtain cross-section based on the door span. A bottom stiffening angle can be added, as well as translational spring elements that simulate a flexible jamb at every wind-lock location. The spring model used was ABAQUS definition Spring Type 2. A Type 2 spring only activates stiffness in the direction of a defined degree-of-freedom (DOF).

4.2 BOUNDARY CONDITIONS

The custom Matlab code applies boundary conditions around the perimeter of the door, including the assignment of springs to simulate wind-lock stiffness. The boundary conditions evaluated in the experimental program are provided in Figure 17. Wind-locks were simulated by fixing the nodes at the wind-lock locations in the out-of-plane 3-direction. Non-linear ABAQUS spring elements were attach to each wind-lock node and assigned the bi-linear spring stiffness in Figure 18 to simulate the effect of the wind-lock gap.

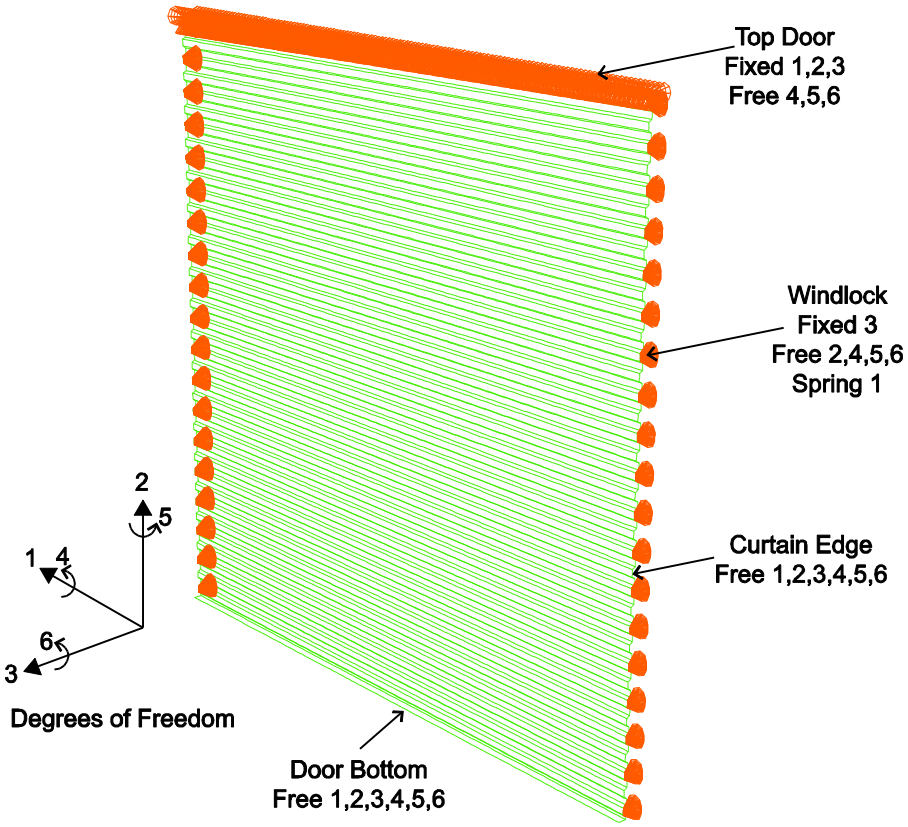

Figure 17. Access door FE boundary conditions

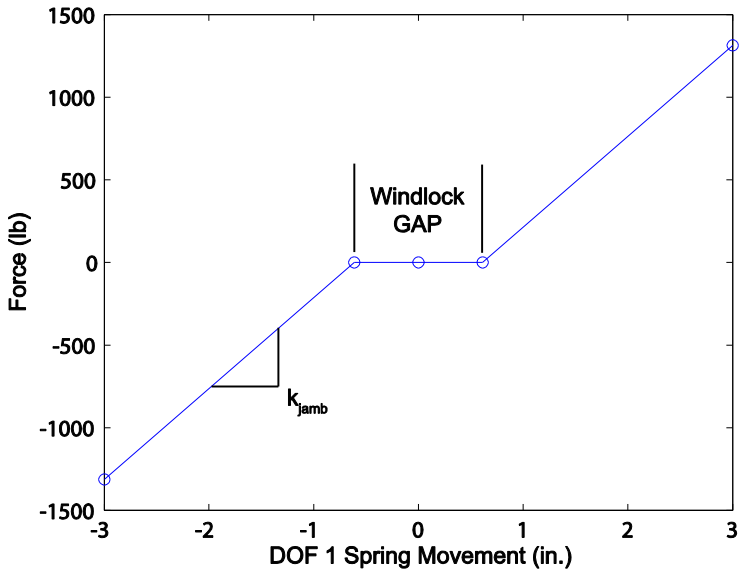

Figure 18. Assumed DOF 1 jamb spring stiffness

4.3 LOADING

Pressure is applied normal to the door curtain in ABAQUS as shown in Figure 19 to be consistent with the vacuum pressure applied in the experimental program. Note that this normal pressure loading may not be the same as a wind pressure on a building, which can be multi-directional and not always normal to the curtain surface.

In ABAQUS, as the pressure increases and the curtain deforms, the pressure direction adjusts to remain normal to the shell surface, i.e., a follower load is specified (Figure 20). Note that as surface area increases under load, for example as the sheet curtain expands, the curtain carries additional force. This loading is different from that assumed in the analytical framework described in Section 2, where the curtain is inextensible and the load magnitude remains constant as the door deflects.

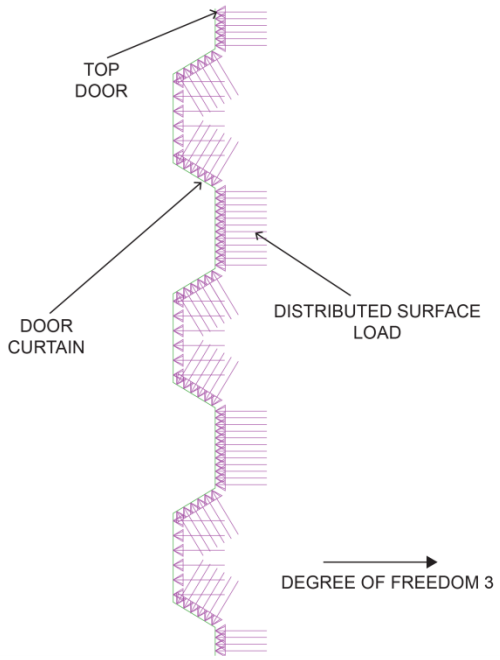

Figure 19. Door surface loading, pressure applied perpendicular to mesh surface

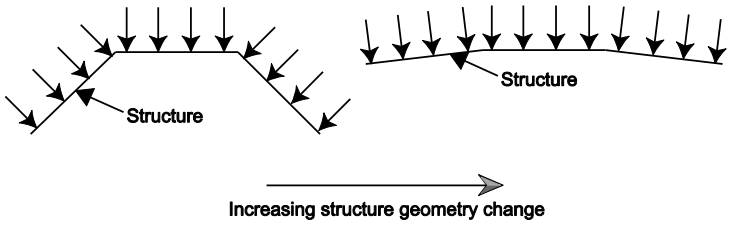

Figure 20. Example of ABAQUS follower load formulation

4.4 SOLUTION ALGORITHM

A nonlinear quasi-static analysis was performed on the door curtain employing the follower surface pressure described in the previous section. The computational solver selected was the Riks arc length method, a modified Newton-Raphson approach that searches the load-deformation space in an arc pattern to identify equilibrium at each load step. Arc length solution methods are good at solving problems where the load-deformation response changes abruptly, e.g., before and after the wind locks engage in an access door.

4.5 COMPARISON OF FE MODEL TO EXPERIMENTS

The modeling protocol described previously was implemented in this section to simulate the load-deformation response of positive pressure test #2 in Gao and Moen (2009). The door dimensions are 10 ft by 10 ft with the curtain profile dimensions provided in Figure 21 and including the stiffening angle across the bottom of the door. The model boundary conditions are consistent with those shown in Figure 17. A bi-linear jamb spring stiffness was employed simulating a wind lock gap of 0.6125 in. (k_{jamb}=0) and then k_{jamb}=529 lb/in. after the wind locks were engaged.

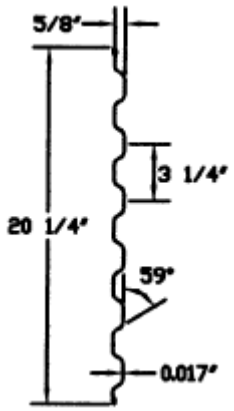

Figure 21. Experimental door curtain dimensions

The simulated and experimental results demonstrate consistent bi-linear load-deformation responses as shown in Figure 22. Before the wind-locks engage, the door resists pressure with curtain bending stiffness. After windlock engagement, the curtain stiffness increases.

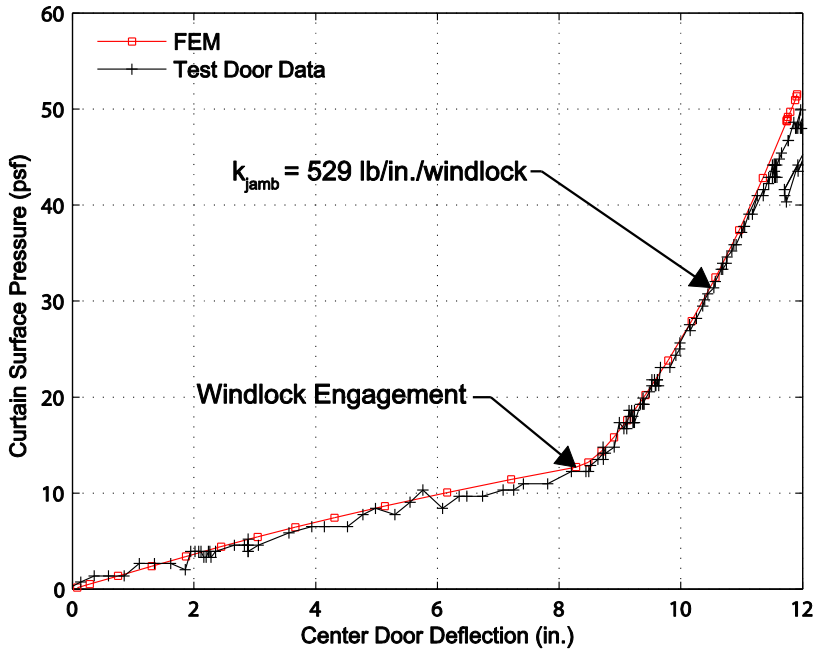

Figure 22. Test center door deflection compared with FEM center door deflection

4.6 Comparison of FE Model to Beam Strip Model

The beam strip approach described in Chapter 2 is used to predict load-deformation response of positive pressure experiment P#2 with the goal of comparing the beam strip predictions to the experimental results. The beam strip model is defined with the following parameters - door span from wind-bar to win-bar, L=120 in., wind lock gap W_{GAP}=0.6125 in., k_{jamb}=529 lb/in., and the curtain moment of inertia, I_w=.0093 in^4 per wind-lock tributary width, and E=30000 ksi.

The load-deformation response from the curtain beam strip model is compared to the experiments in Figure 23, with the beam strip model demonstrating an increasingly stiffer response before the wind locks engage when compared to the experiments and finite element model. The wind locks engage at a smaller curtain out-of-plane deflection in the beam strip model, however after the wind locks engage, the curtain stiffness is consistent with the experiments.

The difference in curtain stiffness before the wind-locks engage between the beam strip model and the experiments (also FE model) is the flattening of the curtain as it is pressurized as shown in Figure 24. To compensate for this reduction in curtain flexural stiffness in the beam strip model, the moment of inertia I_w is reduced by 25% to produce results consistent with the experiments in Figure 25. Even with the moment of inertia correction, windlock engagement

still occurs first in the beam strip model. This trend occurs because the beam strip model assumes axial inextensibility while in the experiments, as the curtain flattens, it increases in length resulting in more out-of-plane deflection before wind-lock engagement. Therefore, the beam strip model will modestly underpredict door deflection. For the test door case considered, the beam strip predicts 11.3 in. while the FE model predicts 12.8 in. at 60 psf as shown in Figure 34.

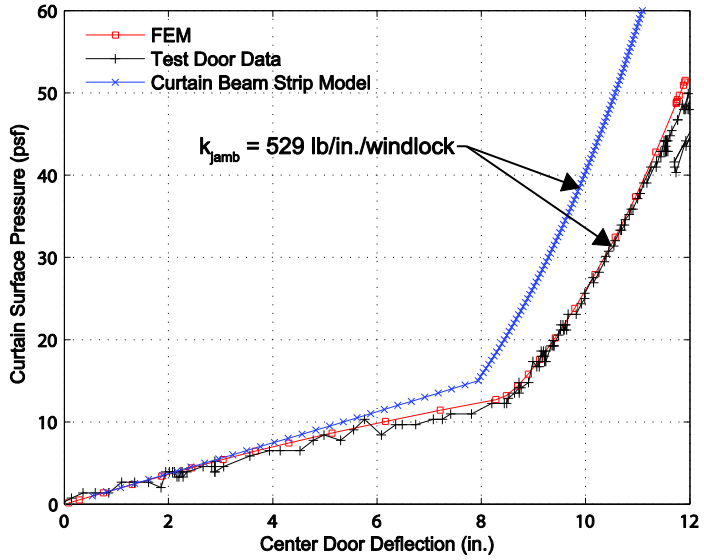

Figure 23. Middle wind-lock, center deflection compared with FEM

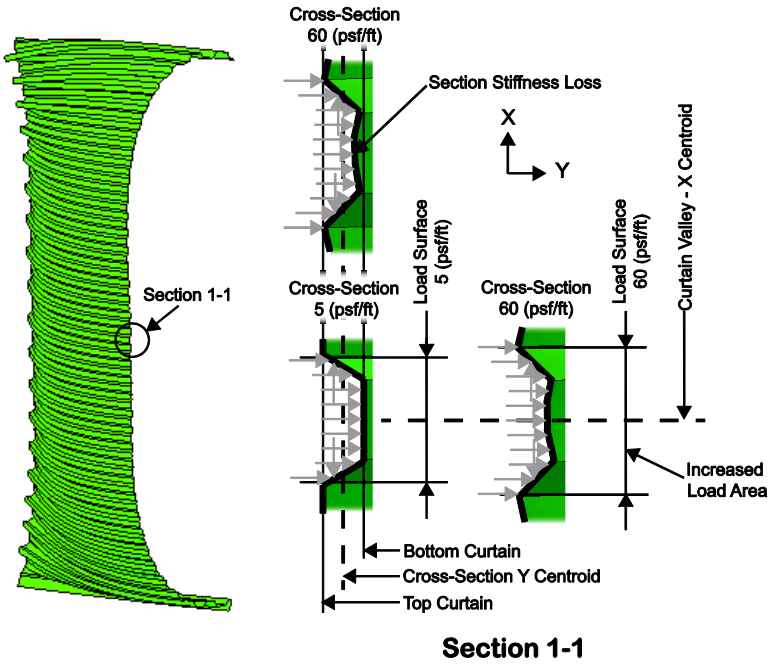

Figure 24. Door curtain moment of inertia loss (section cuts)

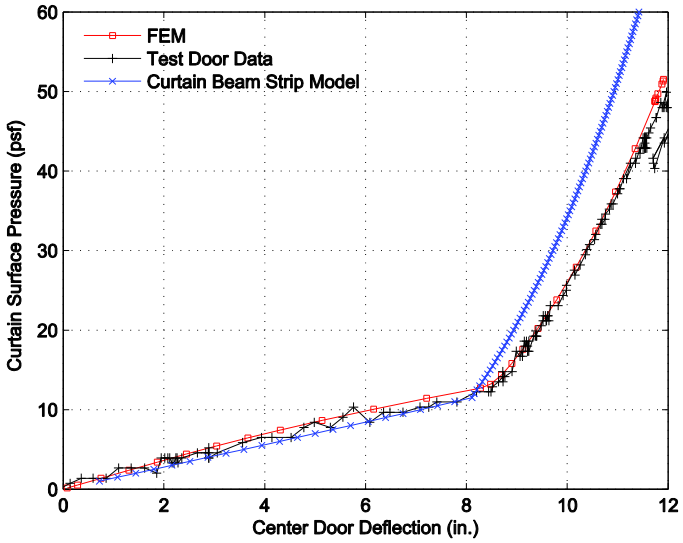

Figure 25. DBCI Series 5000 center door deflection assuming 25% *I* reduction for the beam strip model

The in-plane jamb reaction F_X predicted by the beam strip model and the finite element model demonstrate consistent trends, with the beam strip model underpredicting the forces from 5% to 10% as shown in Figure 26. The out-of-plane jamb reaction F_y is also underpredicted by the beam strip model prediction (Figure 27) relative to the finite element model as pressure increases, because the finite element compensates for the increased loading surface as the curtain flattens , which increases the total applied load to the door. The difference between F_y at 50 psf is approximately 8%, compare 142 lbs to 155 lbs. This load accumulation effect from the flattening door is not considered in the current DASMA approach and is most likely small enough to disregard for typical wind design pressures; however an amplification factor could be added in the future if deemed necessary. It is concluded that the beam strip model is a viable predictor of door behavior and wind-lock forces.

(a)

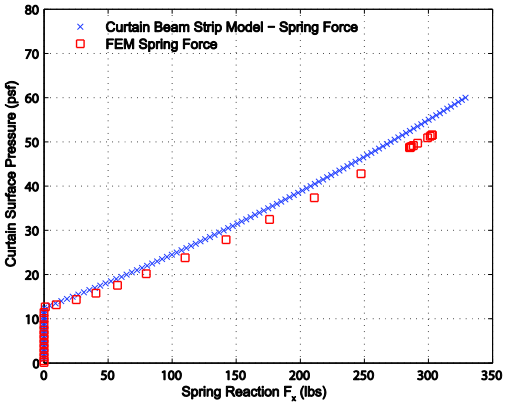

(b)

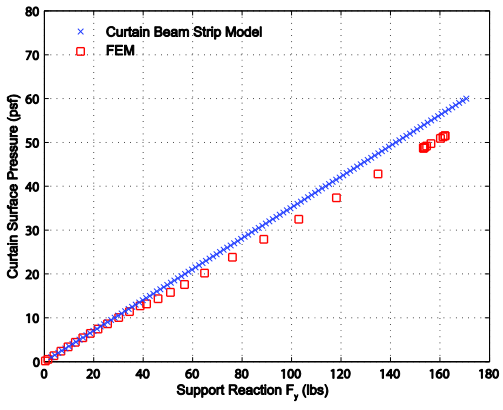

Figure 26. DBCI Series 5000 (a) F_X and (b) F_Y assuming 25% *I* reduction in the beam strip model

4.7 COMPARISON TO DASMA PREDICTION

As discussed in Chapter 1, the current DASMA wind-lock force prediction approach is viable for cases when the jambs are rigid, i.e., when $k_{jamb}=\infty$. To demonstrate the beam strip approach and the DASMA approach produce consistent results, a comparison is conducted with the design inputs summarized in Table 2 considering a pressure of 60 psf. The DASMA wind-lock force per foot of door height was converted to forces per wind-lock to accommodate a comparison, see Appendix C for details of the conversion.

Table 2. Prediction model inputs

Design Input	DASMA	CBSM	Units
Door Pressure	60	60	psf
E	30,000	30,000	ksi
I_w	0.0093	0.0093 * 0.75	in^4
W_s	6.5	6.5	in
L	120	120	in.
W_{GAP}	0.3125	0.3125	in.
k_{jamb}	Not Applicable	4,000,000	lb / in.

The DASMA and beam strip models results are compared in Table 3. The beam strip reaction F_X and F_Y and the out-of-plane door displacement D are within 3% of the DASMA predictions, demonstrating that the beam strip approach is applicable to both flexible and rigid jambs.

Table 3. Results comparison, DASMA vs. curtain beam strip for rigid jambs

Design Output	DASMA (100% of I)	CBSM (75% of I)	% Difference (DASMA/CBSM)
F_x	749	772	-2.98%
F_y	162	163	-0.49%
D	5.30	5.40	-1.85%

5.0 PREDICTION METHOD IMPLEMENTATION

The analytical framework derived in Chapter 2 and validated in Chapter 4 requires a special numerical solver not available in common engineering software. To ensure that the access door analysis approach can be used by engineers, a freely available Matlab tool was developed that implements the curtain beam strip model. A screenshot of the analysis tool is provided in Figure 28 for the experimental test door with flexible jambs. The user can input door dimensions, wind lock spacing, wind lock gap, jamb stiffness, and wind pressure, and obtain a full load-deformation response including out-of-plane door deflection and wind lock forces.

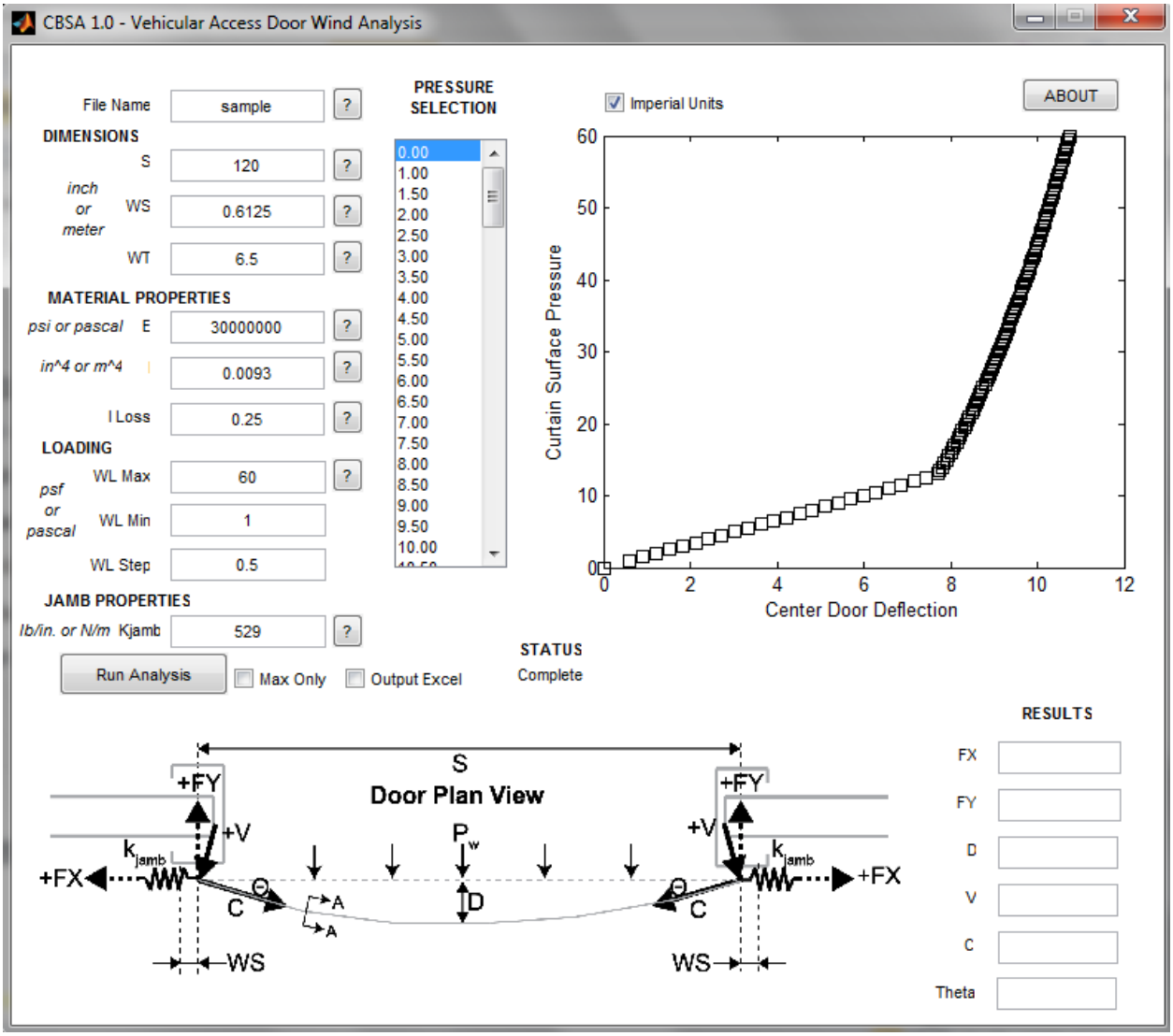

Figure 28. Test door analyzed with CBSA program k_{jamb}=529 lb/in. and W_{GAP} = 0.6125 in

6.0 CONCLUSIONS AND FUTURE WORK

The goal of this research was to develop a fundamental understanding of vehicular access door structural behavior so that more general, accurate analysis tools and design procedures can be provided to the metal building industry. It was demonstrated that the existing DASMA design approach is viable for rigid jambs, e.g., the wind-bar attached directly to a masonry wall, however for flexible jambs, e.g., a cold-formed steel framing system, the wind lock forces were over predicted and the door deflections were under predicted.

A beam strip model based on an Euler-Bernoulli elastica solution was shown to be a viable predictor of primarily one way action of an access door under a wind pressure. The beam strip model overpredicted curtain stiffness and underpredicted out-of-plane forces on the door because of its assumption of axial inextensibility, whereas the real behavior as observed in finite element simulations and experiments was for the door to stretch as pressure is applied. If a reduced curtain moment of inertia is assumed in the beam strip model, the beam strip model produced reliable results.

A primary focus of future work should be the formalization of an access door limit state design approach coupled with the computer analysis tool developed in this research. Based on the recent vehicular access door experiments, limit states that are most likely to control the capacity of a vehicular access door involve the jamb, specifically (1) jamb failure and (2) wind-bar to jamb connection failure. A cold-formed steel jamb can be designed with the wind lock forces calculated with the software in Chapter 5 and cold-formed steel design specifications, e.g., AISI-S100-07. The forces on the jamb connections can also be readily approximated from the design approach and sized appropriately to resist demand forces. Considering serviceability, it is a requirement for the door to roll up after an extreme wind event. Permanent curtain deformation can occur if the door is stretched too much during a wind event. With the curtain deflection predictions provided by the beam strip model, deflection limits could be developed that prevent this plastic deformation.

REFERENCES

ABAQUS (2010). *ABAQUS/Standard Version 6.10* (computer software), www.simulia.com, Providence, RI.

AISC (2003). "Torsion Analysis of Structural Steel Members." *AISC Design Guide Series 9,* Chicago, IL.

Allen, B. (2008). "Series 5000 Door Assembly Details." <http://www.dbci.com/images/PDF/Series_5000.pdf>, (Dec. 12, 2010).

FEMA. (2005a). "Hurricane Charley in Florida: Observations, Recommendations, and Technical Guidance.", *Report FEMA-488*, Federal Emergency Management Agency, United States.

FEMA. (2005b). "Hurricane Ivan in Alabama and Florida: Observations, Recommendations, and Technical Guidance." ,*Report FEMA-489*, Federal Emergency Management Agency, United States.

Gao, T., and Moen, C. D. (2009). "Experimental Evaluation of a Vehicular Access Door Under Hurricane Force Wind Pressures." *Virginia Tech Dept. of Civil and Environmental Engineering, Report No. CE/VPI-ST-09/03.* , Blacksburg, VA.

Gao, T., Moen, C.D. (2010). "Experimental Evaluation of a Vehicular Access Door Subjected to Hurricane Force Wind Pressures*." 20th International Specialty Conference on Cold-Formed Steel Structures, St. Louis, MO.*

Oak Ridge National Laboratory. (2009). "Hurricane Ike - Wind Investigation Report." Oak Ridge National Laboratory.

Matlab (2011a). (computer software), <http://www.mathworks.com/products/matlab/>

NOAA (2011). "NOAA Economics of Hurricane & Tropical Storm Data and Products (Costs)." <http://www.economics.noaa.gov/?goal=weather&file=events/hurricane&view=costs>

RICOWI. (2006). "Hurricane Charley and Ivan Wind Investigation Report." Roofing Industry Committee on Weather Issues, Inc., Powder Springs, GA.

RICOWI. (2007). "Hurricane Katrina Wind Investigation Report." Roofing Industry Committee on Weather Issues, Inc., Powder Springs, GA.

RICOWI. (2009). "Hurricane Ike Wind Investigation Report." Roofing Industry Committee on Weather Issues, Inc., Powder Springs, GA.

SSMA (2010). "Product Technical Information." <http://www.ssma.com/documents/ssmatechcatalog.pdf> (Dec 10, 2010)

Timoshenko, S. P. , Gere, J.M. (1961). *Theory of Elastic Stability*. McGraw-Hill, New York.

APPENDIX A - DASMA PREDICTION METHOD

DBCI Door Series 5000 - used in 8/09 MBMA Research Test

Calculations by Joseph H. Dixon, Jr., 8/19/09

Given:

WL = Wind Load = +/-60.0 PSF

L = Door Width = 10.5 Ft.

P = Slat Pitch = 3.21 In.

I = Slat Moment of Inertia = .00425 In^4 (per slat)

It= Total Moment of Inertia = 12/P x I = . 01589 In^4 (per ft. door ht.)

E = Slat Modulus Elasticity = 30,000,000 P.S.I.

WS = Windlock slip or **Windlock Gap =** .3125 In.

SO= Guide standout or wall to wind bar dimension = 1.037 In.

OFS = Guide dimension wind bar to edge of opening = 1.6875 In.

Determine The Following:

1. **D =** Slat deflection before windlocks engage. (Ft.)
2. **W1 =** Bending load for slat deflection. (Lbs./ft^2)
3. **W2 =** Wind load resisted after windlocks engage. (Lbs./ft^2)
4. **C =** Catenary force for windlock slat tension load. (Lbs./ft. of door ht.)
5. **TH =** Angle of windlock pull. (Deg.)
6. **FX =** Force on windbar inside the guide in the "X" direction. (Lbs./Ft. of door ht.)
7. **FY =** Force on windbar inside the guide in the "Y" direction. (Lbs./Ft. of door ht.)
8. **Pos M =** Positive moment at corner of door opening with +WL interior mount (in-lbs.)
9. **Neg M** = Negative moment at corner of door opening with -WL interior mount (in-lbs)

1. Slat deflection before windlocks engage. (ft.) [based reference 4]

   $$D = (L \times WS)^{1/2} / 4 = .453 \text{ ft.} = 5.433 \text{ in.}$$

2. Bending load for slat deflection. (Lbs./ft^2) [based on reference 1]

   $$W1 = (24 \times E \times It \times D)/ (45 \times L^4) = 6.7 \text{ psf}$$

3. Wind load resisted after wind locks engage. (Lbs./ft^2) [simple sum of wind load forces]

   $$W2 = WL - W1 = 53.3 \text{ psf}$$

4. Forces on wind bar inside the guide in the "X" direction. (Lbs./Ft. of ht.) [based on reference 3]

   $$FX = W2 \times L^2 / 8 \times D = 1621 \text{ lbs./ft of door height}$$

5. Forces on wind bar inside the guide in the "Y" direction. (Lbs./Ft. door of ht.) [sum forces in the y direction equal zero]

   $$FY = WL \times L / 2 = 315 \text{ lbs./ft. of door height}$$

6. Catenary force for wind lock slat tension load. (Lbs./ft of door ht.) [based on reference 3]

   $$C = FX \times (1 + (16 \times (D / L)^2))^{1/2} = 1645 \text{ lbs./ft. of door height}$$

7. Angle of slat to guide. (Deg.) [resultant angle of two know forces]

   $$TH = \text{Cos}^{-1} (Fx / C) = 9.8 \text{ Degrees}$$

8. Wall Moments based on the guide standout value (In-lbs/ ft. of door ht.) [Sum moments about the corner of the opening. See guide drawing for location and direction]

   $$\text{Pos } M = FX \times SO - FY \times OFS = 1150 \text{ in-lbs}$$

$$\text{Neg M} = \text{FX x SO} + \text{FY x OFS} = 2213 \text{ in-lbs}$$

Engineering References

1. Source of the equations for deflection and moment:

AISC Steel Construction Manual, Allowable Stress Design, Uniformly Loaded Beam Unrestrained at the ends

Deflection = 5WL^4/384EI

Moment = WL^2/8

2. Roark & Young Formulae for Stress & Strain, Beams: Flexure of Straight Bars,

for Moment = WL^2/8.

*3. Source of catenary tension equation:

Structural Engineering Handbook, Gaylord & Gaylord, 1989

$T = (QL_w^2/8F) \times (1+16(F/L_w)^2)^{0.5}$

T = Catenary tension, lbs

Q = load, lbs/in

L_w = distance between where windlocks engage, in

F = deflection @ center of slat, in

$H = (QL_w^2/8F)$

H = Horizontal Tension, lbs

*4) Source for Deflection Equation:

Based on Handbook of Engineering Mathematics, American Society of Metals (ASM) (Page 65 For Catenary)

$D = (L_w \times WS)^{1/2} / 4$, where D = Deflection (Ft.), L_w = Door Width (Ft.), WS = Windlock Slip (In.)

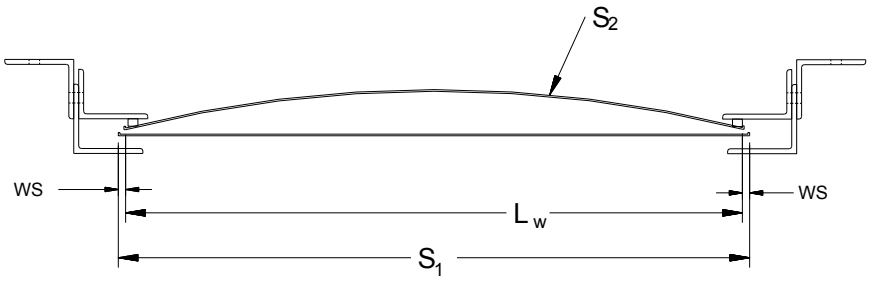

Solve for “D”

$S_1 = S_2$

$S_1 = L_w + 2WS/12$

$S_2 = L_w[\ 1 + 2/3\ (2D/L_w)^2\ ]$

$L_w + (2WS/12) = L_w[\ 1 + 2/3\ (2D/L_w)^2\ ]$ $\quad 2/3 \times 4D^2/L_w^2 = 8D^2/3L_w^2$

$L_w + (2WS/12) = L_w + L_w\ (8D^2/3L_w2\ )$

$2WS/12 = L_w + 8D^2/3L_w - L_w$ Subtract L_w from both sides and factor out L_w

$WS/12 = (8D^2/3L_w) / 2$ Divide by 2 each side = $8D^2/6L_w$

$WS = (8D^2/6L_w)\ 12$ Multiply by 12 each side = $96D^2/6L_w$

$WS = 96D^2/6L_w = 16D^2/L_w$

$D^2 = (L_wWS) / 16$

$D = (L_wWS)^{1/2} / 4$ Square root each side

* For ease of calculations, door width is used in place of L_w

Drawing Illustrating Equation Variables

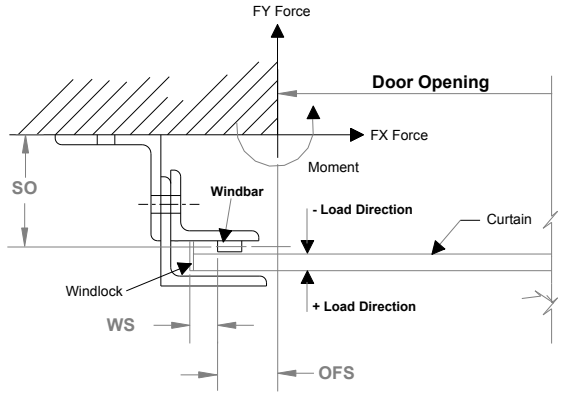

APPENDIX B – DBCI SERIES 5000 DOOR DETAILS

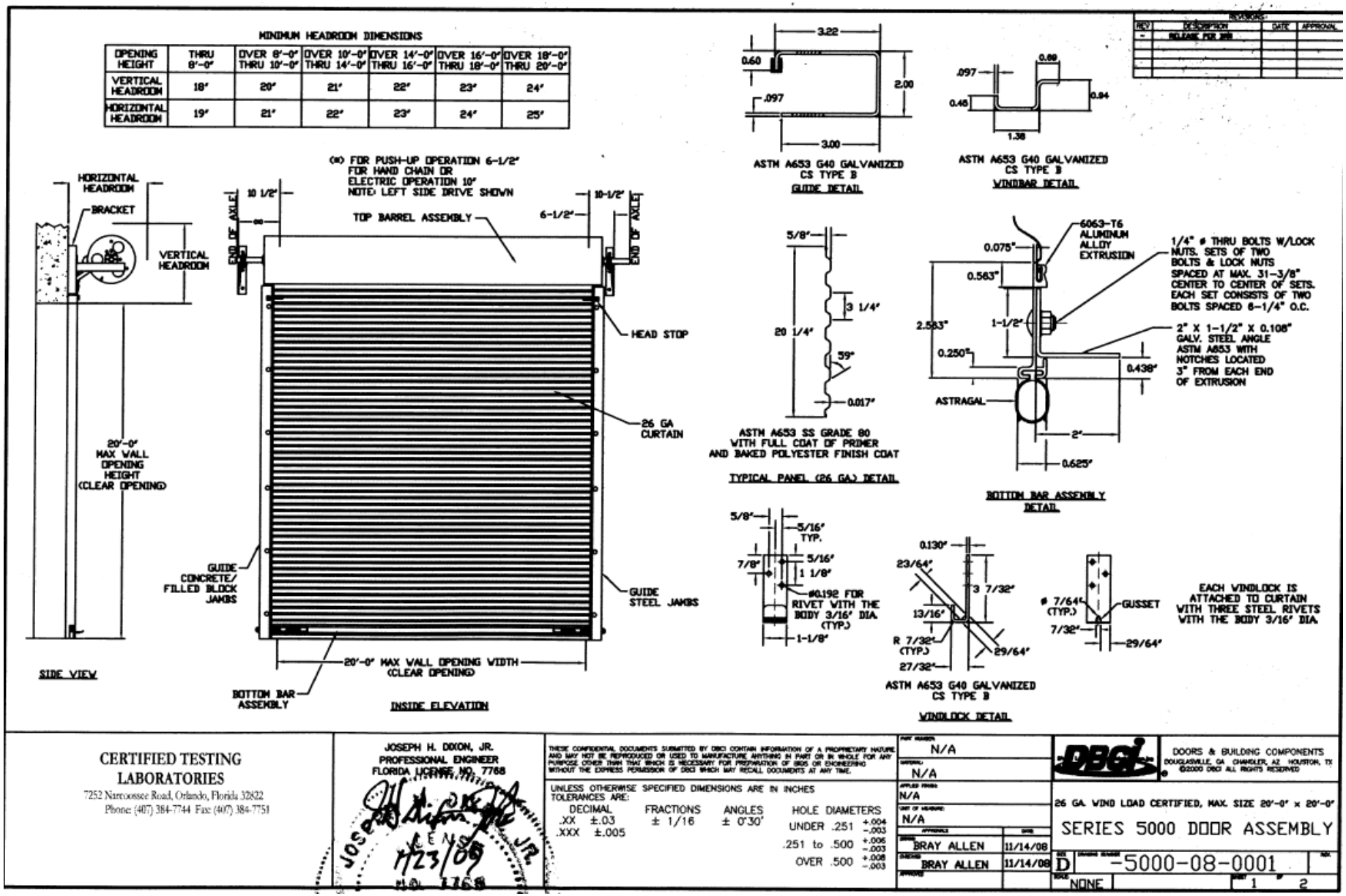

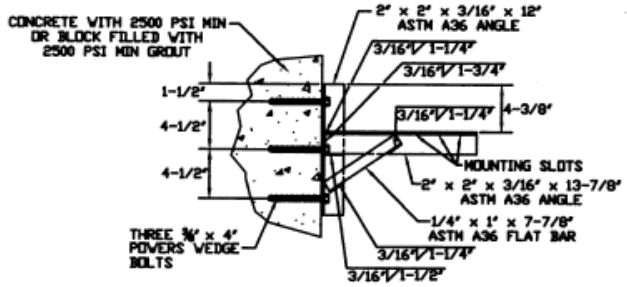

DOOR MOUNTING BRACKET TO MASONRY DETAIL

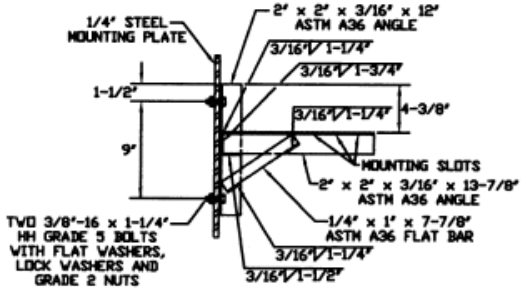

DOOR MOUNTING BRACKET TO STEEL DETAIL

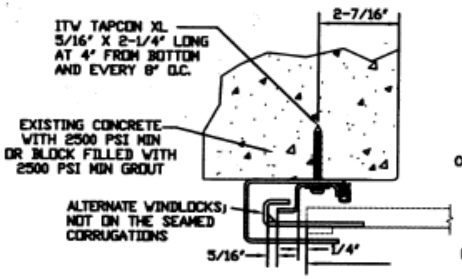

CONCRETE/FILLED BLOCK JAMBS
LH GUIDE MOUNT SHOWN

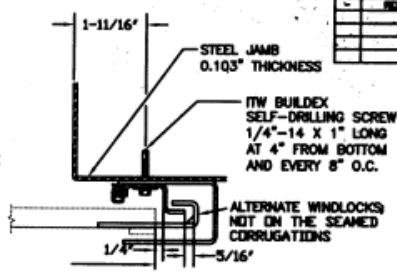

STEEL JAMBS
RH GUIDE MOUNT SHOWN

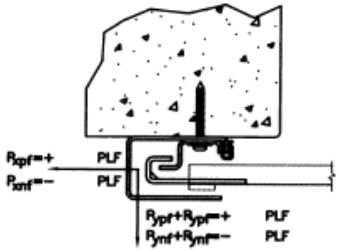

CONCRETE/FILLED BLOCK JAMBS
LH GUIDE MOUNT SHOWN

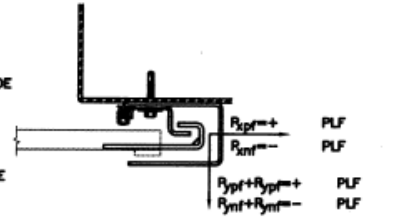

STEEL JAMBS
RH GUIDE MOUNT SHOWN

SUPERIMPOSED LOAD DIAGRAM

DOOR SCHEDULE	
DOOR WIDTH	DESIGN PRESSURE (PSF)
≤ 10'-0"	+39.6
	-67.3
11'-0"	+36.9
	-57.7
12'-0"	+44.1
	-50.2
13'-0"	+38.8
	-44.2
14'-0"	+34.5
	-39.3
15'-0"	+31.0
	-35.3
16'-0"	+28.0
	-32.0
17'-0"	+25.5
	-29.2
18'-0"	+23.3
	-26.7
19'-0"	+21.5
	-24.6
20'-0"	+19.9
	-22.8

GENERAL NOTES:

1. THE DBCI 5000 SERIES ROLL-UP DOOR ASSEMBLY IS DESIGNED IN ACCORDANCE WITH THE FLORIDA BUILDING CODE TO SAFELY RESIST THE WIND LOADS DENOTED BELOW:
   POSITIVE DESIGN LOAD = + 28 PSF;
   NEGATIVE DESIGN LOAD = - 32 PSF.
2. THIS EVALUATION IS BASED ON CERTIFIED TESTING LABORATORIES TEST REPORT NUMBER CTLA-1925W.
3. THE TEST DOOR OPENING SIZE WAS 16'-0" x 7'-0". FOR DIFFERENT OPENING SIZES, THE CORRESPONDING DOOR SIZES ARE CALCULATED TO SAFELY RESIST THE DESIGN LOADS DENOTED IN THE DOOR SCHEDULE.
4. THIS PRODUCT EVALUATION IS GENERIC. IT DOES NOT INCLUDE INFORMATION PREPARED FOR A SPECIFIC SITE.
5. IT IS THE CONTRACTOR'S RESPONSIBILITY TO VERIFY THE STRUCTURAL CAPACITY OF THE SUBSTRATE (JAMB) TO RESIST THE LOADS IMPOSED BY THE ROLL-UP DOOR.
6. ALL DOOR JAMBS (MASONRY OR STEEL) MUST BE DESIGNED ACCORDING TO THE APPLICABLE CODES TO RESIST THE FORCES SHOWN ABOVE.
7. THE DOOR ASSEMBLY SHALL BE ANCHORED IN ACCORDANCE WITH THE PUBLISHED MANUFACTURER'S INSTALLATION INSTRUCTIONS.

CERTIFIED TESTING LABORATORIES
7252 Narcoossee Road, Orlando, Florida 32822
Phone: (407) 384-7744 Fax: (407) 384-7751

JOSEPH H. DIXON, JR.
PROFESSIONAL ENGINEER
FLORIDA LICENSE NO. 7768
LICENSE 11/23/08 NO. 7768

UNLESS OTHERWISE SPECIFIED DIMENSIONS ARE IN INCHES
TOLERANCES ARE:
DECIMAL .XX ±.03 .XXX ±.005
FRACTIONS ± 1/16
ANGLES ± 0°30'
HOLE DIAMETERS UNDER .251 +.004 −.003; .251 to .500 +.006 −.003; OVER .500 +.008 −.003

PART NUMBER	N/A
MATERIAL	N/A
APPLIED FINISH	N/A
UNIT OF MEASURE	N/A
APPROVALS	DATE
DRAWN BRAY ALLEN	11/14/08
CHECKED BRAY ALLEN	11/14/08
APPROVED	

DBCI DOORS & BUILDING COMPONENTS
DOUGLASVILLE, GA CHANDLER, AZ HOUSTON, TX

26 GA. WIND LOAD CERTIFIED, MAX. SIZE 20'-0" x 20'-0"

SERIES 5000 DOOR ASSEMBLY

SIZE D | DRAWING NUMBER 5000-08-0001 | REV.
SCALE NONE | SHEET 2 OF 2

APPENDIX C- DASMA METHOD

The following calculation is equivalent to that in Appendix A, except the catenary forces are calculated per wind-lock instead of per ft of door.

DASMA Door Calculation Test Door

- input parameters

$WL := 60$ psf

$L := 10$ ft *door width

$P := 3.25$ in *slat pitch

$WT := \frac{6.5}{12} = 0.542$ *Wind Locks per Foot of Door

$I := .00425$ *slat moment of inertia

$It := \frac{12}{P} \cdot I = 0.016$ *total moment of inertia per foot of door height

$E := 30000000$ modulus

$WS := 0.3125$ in *windlock slip gap

- Dasma calculation as outlined in Appendix II

Part 1 - Slat Deflection before windlocks enagages based on arc approximation.

$$D := \frac{(L \cdot WS)^{0.5}}{4} = 0.442 \text{ ft} \qquad D \cdot 12 \rightarrow 5.303 \text{ inches}$$

Part 2 - Bending Load for slat deflection based on euler beam theory

$$D = \frac{w \cdot 45 \cdot L^4}{24 \cdot E \cdot It} \text{ solve, } w \rightarrow 11.096 \frac{\text{lb}}{\text{ft}^2}$$

$$W1 := \frac{D \cdot 24 \cdot E \cdot It}{45 \cdot L^4} \rightarrow 11.096 \ \frac{lb}{ft^2}$$

Part 3 - Wind load resisted after wind locks engage

$$W2 := WL - W1 \rightarrow 48.904 \quad psf$$

Part 4 - Forces on wind bar inside the guide in the "X" direction. ARCH reaction force.

$$FX := W2 \cdot \frac{L^2}{8D} \cdot WT \rightarrow 749.239 \ lbs$$

Part 5 - Forces on wind bar inside the guide in the "Y" direction.

$$FY := WL \cdot \frac{L}{2} \cdot WT = 162.5 \qquad \frac{lb}{windlock}$$

Part 6 - Catenary force for windlock. Based on cable equation.

$$C := FX \cdot \left[1 + \left[16 \cdot \left(\frac{D}{L}\right)^2\right]\right]^{0.5} = 760.856 \quad lbs$$

Part 7 - Angle of slat to guide.

$$TH := acos\left(\frac{FX}{C}\right) \cdot \frac{180}{\pi} = 10.025 \ deg$$

Part 8 - Forces per windlock

$$FX \rightarrow 749.239 \ lbs$$

$$FY \rightarrow 162.5 \quad lbs$$

APPENDIX D - MATLAB CODE

```
function output = CBSM(OutputID, Pressure, SpanL, Kjamb, E, Ixx, Ireduction, WindlockTribLength, WindLockGap)
%**************LOOK AT ODE**************

%Index 1 = Output Pressure Applied
%Index 2 = Output Center Door Deflection - used to check excessive movement
%Index 3 = Output Edge Rotation (radians)- used to check windlock unhinging
%Index 4 = RF1 Windbar Jamb Reaction     - used to design jamb connection
%Index 5 = RF3 Windbar Jamb Reaction     - used to design jamb connection
%Index 6 = Beam Strip Curtain Shear @ Support
%Index 7 = Beam Strip Curtain Axial Force (Catenary) @ Support)
%Index 8 = Edge Support Movement (Jamb Movement)


%%%%%%%%%%%%%%%%%%%%%%%%%%%%%%%%%%%Input%%%%%%%%%%%%%%%%%%%%%%%%%%%%%%%%%%%%%%%
%%%
B = SpanL/2;                          %find half span for sol method
E = E*1000;                           %change E from ksi (input)
                                      %to psi (needed in program)

WindLockSlipGrab = WindLockGap;           %wind lock gap for door (inches)
global WindLockSlipLimit;                %make this variable accessable by all functions
WindLockSlipLimit = (WindLockSlipGrab/B);   %non-dimensional windlockslip limit

global WindlockTribArea;                 %make this variable accessable by all functions
WindlockTribArea = WindlockTribLength/12;   %cetner to center spacing of windlock (units = feet)

  %USE THIS Ix for constant Ix applied
  I = Ixx*Ireduction;                  %moment of inertia for lock trib length

  W = Pressure;                        %Start Value for WindLoading (psf)
  WindLoad = W*WindlockTribArea/12;       %scale down PSF to applied section PSF

  %Find Out If Windlock Engage
  K=.0001;                             %Run Program With No Stiffness
  %%%%%%%%%%%%%%%%%%%%%%%%%%%%SOLVER%%%%%%%%%%%%%%%%%%%%%%%%%%%%%%%%%%%%%%%%%%%
  %Non-Dimensional
  global w;                            %script w
  global k;                            %script k
  global windlockslip;
  windlockslip = 0;                    %windlock slips is always zero for this run
  w=WindLoad*B^3/(E*I);
  k=K*B^3/(E*I);
  P = 0.1;                             %initial guess for unknown value
  solinit = bvpinit(linspace(0,1,100),@mat4init,P);
                                       %solve boundary condition problem
  sol = bvp4c(@mat4ode,@mat4bc,solinit);
                                       %fprintf('The P Horizontal Force (lbs): %7.3f.\n',...
                                       %sol.parameters*(E*I)/(B^2))
  xint = linspace(0,1);                %space to look at from t = 0 to t = 1
  Answer = deval(sol,xint);            %determine answers over space interval

  %check to see if windlocks engage
  windlockslip = 1 - Answer(1,100);       %find out how much edge moved in the X direction

  if windlockslip < WindLockSlipLimit
  %windlocks have not egaged so output data
  switch OutputID
    case 1
      output =  W;
    case 2
      output =  Answer(2,1)*B;        %Hold Center Delfection Output for This Load
    case 3
      output =  Answer(3,100);        %Hold Beam Roation
    case 4

      output = (B - (Answer(1,100)*B))*K;    %output RF1
      if output < 0.001                 %if output is just method error
        output = 0;
      end
```

```
        case 5
          %Calculate Beam RF3 Reaction
          endbeamshear = -(WindLoad*B)*cos(Answer(3,100))+(sol.parameters*(E*I)/(B^2))*sin(Answer(3,100));
          endaxialforce = (-sol.parameters*(E*I)/(B^2)+sin(Answer(3,100))*endbeamshear)/(cos(Answer(3,100)));
          YBeamReaction = -cos(Answer(3,100))*endbeamshear-sin(Answer(3,100))*endaxialforce;
          output = YBeamReaction;
        case 6
          %Find Out Beam End Shear
          endbeamshear = -(WindLoad*B)*cos(Answer(3,100))+(sol.parameters*(E*I)/(B^2))*sin(Answer(3,100));
          output =  endbeamshear; %Hold Beam Shear
        case 7
          %Find Out End Axial Force
          endbeamshear = -(WindLoad*B)*cos(Answer(3,100))+(sol.parameters*(E*I)/(B^2))*sin(Answer(3,100));
          endaxialforce = (-sol.parameters*(E*I)/(B^2)+sin(Answer(3,100))*endbeamshear)/(cos(Answer(3,100)));
          output =  endaxialforce; %Hold End Beam Axial Force
        case 8
          output = (B - (Answer(1,100)*B)); %output edge movement
    end

else
%windlocks have engaged so rerun model with new stiffness
%ANOTHER RUN WITH STIFFNESS
W = Pressure;                           %reset pressure to applied pressure
I = I;                                %Keep Last I applied to curtain
K=Kjamb;                                %apply jamb stiffness
WindLoad = W*WindlockTribArea/12;                %lbs per inch
%%%%%%%%%%%%%%%%%%%%%%%%%%%%SOLVER%%%%%%%%%%%%%%%%%%%%%%%%%%%%%%%%%%%%%%%%%%%%%
%%%%
                               %Non-Dimensional
B = SpanL/2;
global w;
global k;
w=WindLoad*B^3/(E*I);
k=K*B^3/(E*I);
windlockslip = WindLockSlipLimit;               %set windlock gap to closed
P = 0.1;                              %initial guess for unknown value
solinit = bvpinit(linspace(0,1,100),@mat4init,P);
                               %solve boundary condition problem
sol = bvp4c(@mat4ode,@mat4bc,solinit);
xint = linspace(0,1);                        %space to look at
Answer = deval(sol,xint);

switch OutputID
    case 1
        output =  W;
    case 2
        output =  Answer(2,1)*B;                        %Hold Center Delfection Output For Load
    case 3
         output =  Answer(3,100); %Hold Beam Roation
    case 4
         output =  (B - (Answer(1,100)+windlockslip)*B)*K;          %Hold RF1 Reaction
    case 5
        %Calculate Beam Y Reaction
        endbeamshear = -(WindLoad*B)*cos(Answer(3,100))+(sol.parameters*(E*I)/(B^2))*sin(Answer(3,100));
        endaxialforce = (-sol.parameters*(E*I)/(B^2)+sin(Answer(3,100))*endbeamshear)/(cos(Answer(3,100)));
        YBeamReaction = -cos(Answer(3,100))*endbeamshear-sin(Answer(3,100))*endaxialforce;
        output = YBeamReaction;
    case 6
        %Find Out Beam End Shear
        endbeamshear = -(WindLoad*B)*cos(Answer(3,100))+(sol.parameters*(E*I)/(B^2))*sin(Answer(3,100));
        output =  endbeamshear; %Hold Beam Shear
    case 7
        %Find Out End Axial Force
        endbeamshear = -(WindLoad*B)*cos(Answer(3,100))+(sol.parameters*(E*I)/(B^2))*sin(Answer(3,100));
        endaxialforce = (-sol.parameters*(E*I)/(B^2)+sin(Answer(3,100))*endbeamshear)/(cos(Answer(3,100)));
        output =  endaxialforce; %Hold End Beam Axial Force
    case 8
        output =  (B - (Answer(1,100)+windlockslip)*B);
end
end

% ------------------------------------------------------------
```

```
function dydx = mat4ode(x,y,P)
global w;
dydx = [cos(y(3))
        sin(y(3))
        y(4)
        -w*x*cos(y(3)) + P*sin(y(3))];
% --------------------------------------------------------------
function res = mat4bc(ya,yb,P)
global k;
global windlockslip;
%y(1) = y1 or X(t)
%y(2) = y2 or Y(t)
%y(3) = y3 or theta(t)
%y(4) = y4 or moment(t) y4' shear(t)
res = [  ya(1) %@ beggining value
         ya(3)
         yb(2) %@ ending value
         yb(1)-1+(P/k)+windlockslip;
         yb(4)]; %moment at the end of beam must be 0
% --------------------------------------------------------------
function yinit = mat4init(x)  %return column matrix yinit for guess y and y'
yinit = [  1  %guess for X(t)
           1  %guess for Y(t)
           x^2 %guess for theta(t)
           1-x^2 %guess for moment(t)
            ];
```

APPENDIX E - SHELL ELEMENT COMPARISONS

ELEMENT TYPES

ABAQUS offers several finite element types. Elements include 3D continuum, 3D shell, 2D truss, 2D frame and 2D shell elements. Considering discussed door behavior, a quasi 3D shell/plate element is most applicable for curtain modeling. An explanation of why this element type was chosen follows below.

CURTAIN SHELL ELEMENT

Consider a small section of door curtain. This portion would be subjected to a uniform surface pressure. Possibly internal plate edge moments and membrane force (Catenary Force) may develop as shown in Figure.

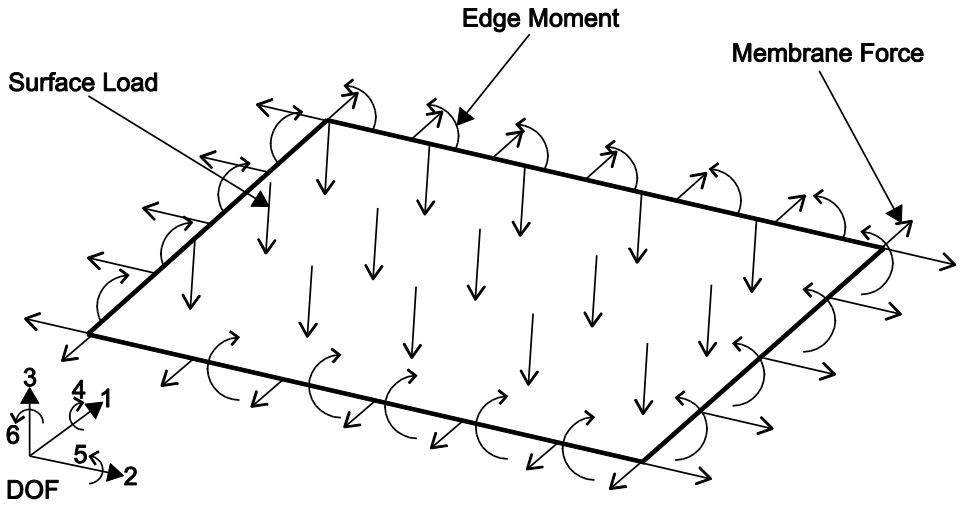

Figure1. Forces applied to a small piece of door curtain

Within Figure, it can be deduced that cross-sectional thickness area, plane *1-3* and *2-3* is much less than the area of applied pressure, surface *1-2*. Therefore, stress in the *3* direction is negligible as compared to developed bending stresses within cross-section planes *1-3* and *2-3*. These assumptions fall in line with the assumptions of thin plate theory which include; (1) straight planes normal to the mid-surface remain straight after deformation, (2) straight planes normal to the mid-surface remain normal to the mid-surface after deformation, (3) the thickness of the plate does not change during deformation.

The developed membrane force of the shell element is attributed to the axial force developed along the door curtain mid-plane when windlocks engage. This statement aligns itself with shell theory. Shell theory includes all assumptions of plate theory but includes effects of

axial force within the element. Therefore, the door curtain should be modeled using one of ABAQUS's quasi 3D shell elements.

BEHAVIOR OF ABAQUS SHELL ELEMENTS

This research pertains to thin steel sheet geometries, 20 to 26 gauge thicknesses. Finite shell element research has been performed with success using the following ABAQUS standard elements, Table 1. Table 1 and Figure 26 identify important formulation aspects of each element.

Table 1. ABAQUS Shell Element Comparison

Element Type		Translation DOF	Rotation DOF	Plate Analysis	Small Strain
S4	Linear	*1 2 3*	*4 5 6*	Thick OR Thin	NO
S4R	Linear	*1 2 3*	*4 5 6*	Thick OR Thin	NO
S4R5	Linear	*1 2 3*	*4 5*	Thin	YES
S8R	Quad	*1 2 3*	*4 5 6*	Thin	YES
S9R5	Quad	*1 2 3*	*4 5*	Thin	YES
STRI3	Linear	*1 2 3*	*4 5*	Thin	YES

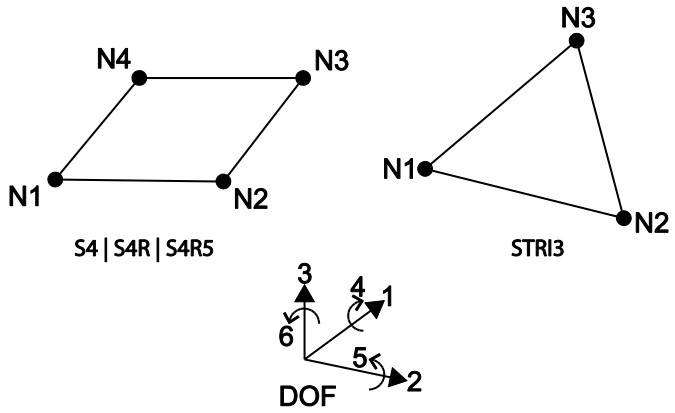

Figure 26. Abaqus S4 element node detail shown left. Abaqus STRI3 element node detail shown right.

Element selection is important because some elements will include the effect of transverse DOF 3 shear deformation and shell thickness change. Both shear deformation and shell thickness change can affect overall door deflection of the developed door model. Hence, *RX* and *RY* will be inaccurately predicted. From the research scope, it is apparent that span to curtain depth ratio will be large. Typical door spans are in the range of 10 to 20 feet. In this range most deformation will occur from bending strain of *DOF 1* and *2*, Figure. Therefore, it is not a requirement to select an element which includes insignificant shear deformation in the

direction of surface loading, *DOF 3*, Figure 26. However, including this effect will increase solution accuracy.

The assumption of small strain relates to the change in thickness of the shell element. For small strain elements, the thickness of material remains constant throughout problem solving. Poison's effect is ignored. The thickness of shell before loading is the same after it has been loaded. Therefore, small strain elements are less accurate at predicting nodal movement as elements capable of handling large strains such as element S4.

Moreover, it is important to find an element that will support membrane forces (Catenary Curtain Force). Membrane forces occur in DOF *1* and *2*. When the curtain is restrained on jamb edges from windlock engagement, the door develops membrane force. This force will be tensile and will stiffen the deflection response of the door system resulting in a slower rate of deflection for each increment of pressure. All elements shown in Table are shell elements. Shell elements are formulated to include membrane forces.

Because each element uses a different formulation the chosen shell behavior must be verified before use. A shell element comparison was completed. Six different elements were used to mesh a 10 in. by 10 in. steel plate of 0.5 in. thicknesses. Mesh density was chosen by analyzing each plate model until the center node deflection converged to a common value for a decrease in element size. Figure 37 shows the mesh density of 0.5 in. by 0.5 in. used for all shell elements.

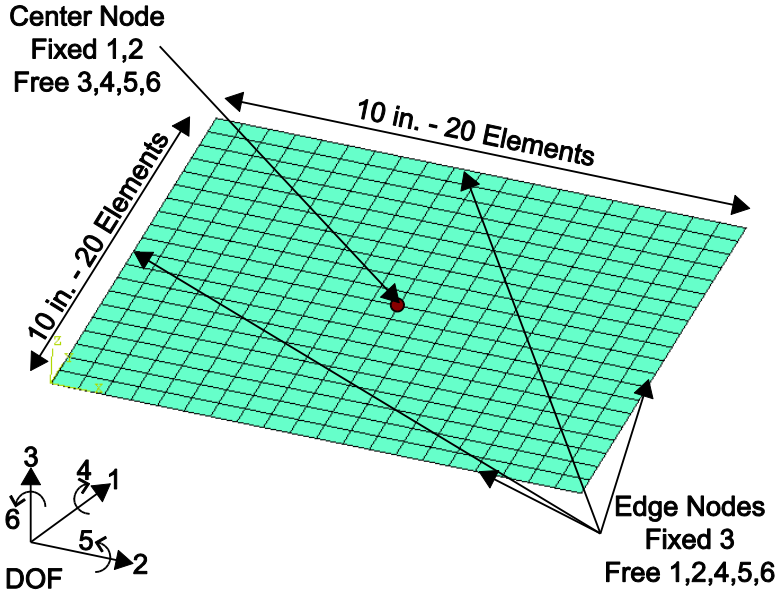

Figure 37. Chosen mesh density rendering, 1 element for each 0.5 inch

An exact Navier-Stokes classical plate solution is provided in Appendix **X** based on Kirchhoff thin plate theory neglecting *DOF 3* shear deformation (Figure 37). This solution was used to verify the performance of each chosen shell element. Comparison plots are shown in Figure 48 through Figure 79.

Element STRI3 neglects shear deformation. Therefore, behavior of STRI3 behavior is verified by the exact match of solution output with classical solution in Figure 79. Elements S4 and S4R5 both include effects of shear deformation. Behavior is verified by the over prediction of center plate deflection as shown in Figure. Tensile stiffening due to membrane force was verified by applying a membrane load to the plate element in axial DOF *1* and *2*. The stiffening effect is shown in Figure by a decrease in central plate deflection with applied axial edge force.

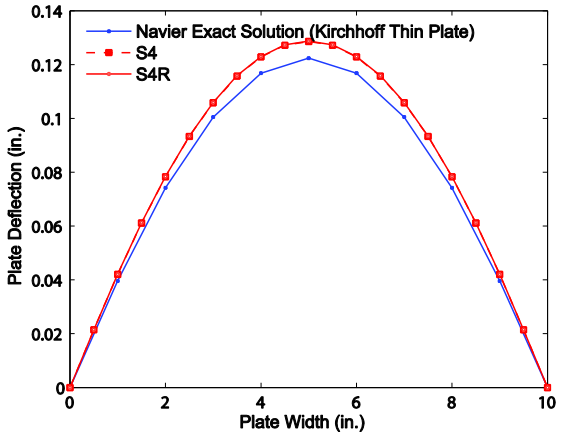

Figure 48: Exact plate solution versus ABAQUS element S4 and S4R

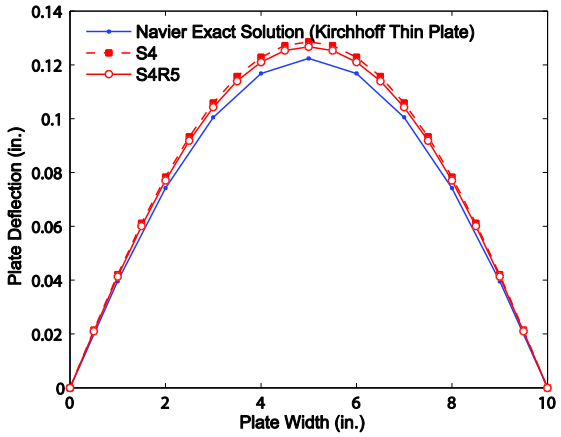

Figure 5: Exact plate solution versus ABAQUS element S4 and S4R5

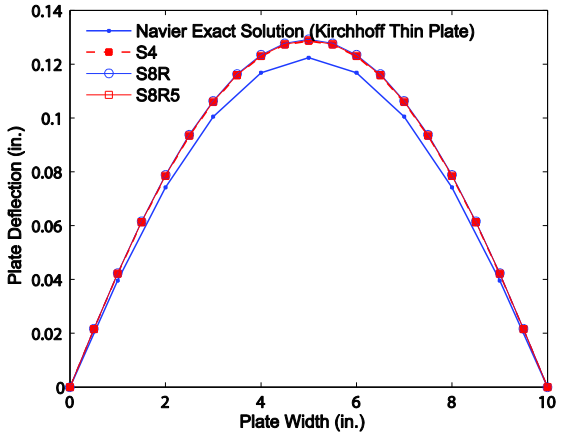

Figure 6: Exact plate solution versus ABAQUS element S4, S8R and S8R5

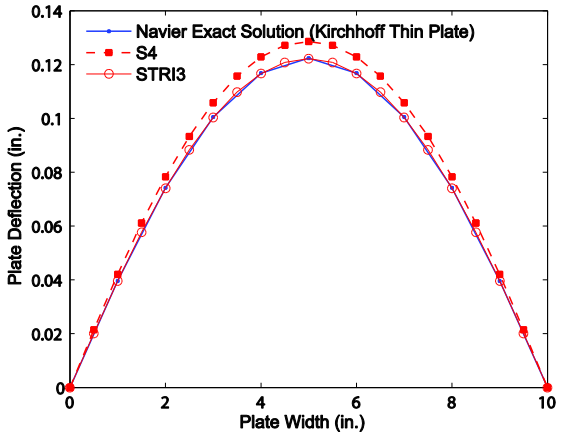

Figure 79: Exact plate solution versus ABAQUS element S4 and STRI3

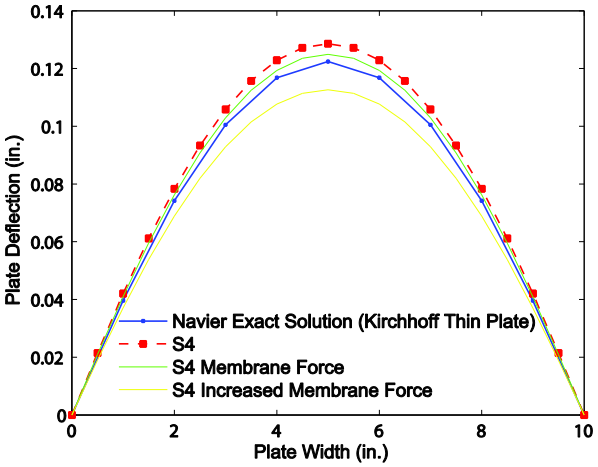

Figure 8: Shell Element S4 Plate with Edge Membrane

APPENDIX F – NAVIER-STOKES EXACT PLATE SOLUTION

Simply Supported Square Plate

$E := 29000\ ksi \qquad \nu := 0.3 \qquad h := 0.5\ in \qquad a := 10\ in \qquad b := 10\ in$

Assumptions

- Material is homogenous, isotropic, and linear elastic'
- Plate is initially flat
- Small Deflections
- Kirchoff's hypothesis - lines initially normal to middle surface remain unstrained and normal to middle surface
- Vertical shear strains are negligible
- Middle Surface is a neutral surface (does not extend)
- Normal stresses are relatively small

Navier's Solution

$$\frac{\partial^4 w}{\partial x^4} + 2\frac{\partial^4 w}{\partial x^2 \partial y^2} + \frac{\partial^4 w}{\partial y^4} = \frac{p}{D}.$$

$$D := \frac{E \cdot h^3}{12 \cdot \left(1 - \nu^2\right)} = 331.96$$

$$w(x, y, q_o) := \frac{1}{D \cdot \pi^6} \cdot \sum_{m=1}^{1000} \sum_{n=1}^{1000} \left[\frac{16 \cdot q_o \cdot \sin\left(\frac{\pi \cdot m}{2}\right)^2 \cdot \sin\left(\frac{\pi \cdot n}{2}\right)^2}{m \cdot n \cdot \left[\left(\frac{m}{a}\right)^2 + \left(\frac{n}{b}\right)^2\right]^2} \cdot \sin\left(\frac{m \pi x}{a}\right) \cdot \sin\left(\frac{n \pi y}{b}\right) \right]$$

$$\Delta_{max} := w\left(\frac{a}{2}, \frac{b}{2}, 1\right) = 0.1224\ in$$

Rule of Thumb Check (Theory Accuracy)

Thin $h = 0.5\ in < 0.1a = 1\ in$ and $0.1b = 1\ in$ Therefore OK

Deflections

$\Delta_{max} = 0.1224\ in$

$\Delta_1 := w\left(1, \frac{b}{2}, 1\right) = 0.0396 \quad in$

$\Delta_2 := w\left(0.2a, \frac{b}{2}, 1\right) = 0.0742 \quad in$

$\Delta_3 := w\left(0.3a, \frac{b}{2}, 1\right) = 0.1005 \quad in$

$\Delta_4 := w\left(0.4a, \frac{b}{2}, 1\right) = 0.1168 \quad in$

$\Delta_5 := w\left(0.500a, \frac{b}{2}, 1\right) = 0.1224 \quad in$